JOURNAL OF PETROLOGY | VOLUME 44 | NUMBER 6 | PAGES 995–1029 | 2003

Processes and Conditions During Contact Anatexis, Melt Escape and Restite Formation: the Huntly Gabbro Complex, NE Scotland

G. T. R. DROOP[1]*, J. D. CLEMENS[2] AND D. J. DALRYMPLE[1]

[1]DEPARTMENT OF EARTH SCIENCES, UNIVERSITY OF MANCHESTER, MANCHESTER M13 9PL, UK
[2]SCHOOL OF EARTH SCIENCES AND GEOGRAPHY, CEESR, KINGSTON UNIVERSITY, PENRHYN ROAD, KINGSTON-UPON-THAMES KT1 2EE, UK

RECEIVED DECEMBER 15, 2001; ACCEPTED DECEMBER 2, 2002

*The Huntly Gabbro is one of a suite of large, Ordovician, syn-orogenic, mid-crustal, layered, mafic intrusions, emplaced into Proterozoic metaclastic rocks of NE Scotland soon after the thermal peak of static, high-*T*, low-*P *regional metamorphism. This gabbro and its associated contact metamorphic rocks illustrate a variety of processes operating during contact anatexis and subsequent melt segregation and extraction. These processes may closely mirror those occurring at much larger scales in the deep crust during high-grade regional metamorphism and the generation of granitic magmas. The emplacement of the Huntly mafic magma resulted in high-grade contact metamorphism and, locally, anatexis of metapelites, leading to the formation of migmatites. The migmatites and country-rock schists were studied to establish the physical conditions of metamorphism and anatexis, the nature of the melting reactions, the compositions of the melts produced, and the extent to which melting was a closed- or open-system process. The country-rock schists immediately to the south of the Huntly Complex contain mineral assemblages characteristic of the regional andalusite zone. Thermobarometry of an andalusite schist yields regional metamorphic conditions of 537 ± 42°C and 0·27 ± 0·12 GPa, consistent with previously published* P–T *estimates. The contact metamorphic rocks include sillimanite hornfelses, metatexites and diatexites. The metatexites consist of cordierite–K-feldspar hornfels melanosomes and K-feldspar-rich garnetiferous leucosomes. The diatexites consist of schollen of fine-grained granoblastic hornfels and metatexite suspended in igneous-textured matrix rocks composed of abundant sub/euhedral garnet, cordierite, plagioclase and, locally, orthopyroxene, with minor interstitial biotite, K-feldspar and quartz. The hornfels melanosomes and schollen retained their structural integrity during partial melting, but the matrix rocks did not. In the highest-grade diatexites, the assemblage Grt + Opx + Crd + Hc + Pl characterizes both the hornfels schollen and the sub/euhedral minerals of the matrix rocks. Application of phase equilibria to Opx-bearing rocks yields estimated peak-metamorphic conditions of 900 ± 50°C, 0·45 ± 0·1 GPa and* $a_{H_2O} < 0{\cdot}3$*. The pressure estimate implies an emplacement depth of ~16 ± 3 km. The prograde* P–T *path of contact-metamorphic rocks had a low, positive* dP/dT *slope, indicating that the gabbro intrusion increased the lithostatic load on the country rocks by overplating. Pseudomorph textures involving Al-silicates provide strong evidence that the diatexites evolved from andalusite schists via a sillimanite hornfels stage. Mineralogical changes reflect a sequence of dehydration reactions, followed by fluid-absent partial-melting reactions involving biotite breakdown. It was the fluid-absent reactions that generated the sub/euhedral minerals in the diatexites, as peritectic phases. In many of the highest-grade diatexites, quartz-free anhydrous solid assemblages were produced via reactions such as Bt + Sil + Grt = Crd + Hc + Kfs + melt and Bt + Grt + Crd = Opx + Hc + Kfs + melt. Whole-rock major-element geochemical studies indicate that the Opx–Crd hornfelses and diatexite matrices are depleted in Si and K relative to their schist protoliths. Mass-balance calculations indicate that (1) the Opx–Crd hornfels xenoliths represent solid Ca-, Mg-, Fe-, Al-, Na-rich residues left after extraction of ~60% melt; (2) the Opx-bearing diatexite matrix rocks are also residual, and represent restite-enriched crystal–liquid mushes left after extraction of ~55% melt; (3) the Opx-free diatexite matrix rocks probably represent restite-enriched mushes that retained a higher proportion of residual melt; (4) the anatectic melts were of* H_2O*-undersaturated, peraluminous,*

*Corresponding author. E-mail: Giles.Droop@man.ac.uk

low-Ca, potassic granite composition. Melt compositions and proportions were confirmed experimentally by partially melting local metapelite samples at 900°C and 0·5 GPa, under fluid-absent conditions. The similarity between the compositions of calculated and experimental melts implies that the melts underwent little or no fractional crystallization before their expulsion. At many localities, a large proportion of the melt escaped from the sites of its generation. Segregation of melt from restite was probably achieved through gravity-driven processes. The fugitive granitic melts did not mix with the gabbroic magma to any great extent, although contamination of mafic magma occurred locally, leading to the generation of biotite-bearing gabbros. The fugitive melts probably contributed to the contemporaneous 'Grampian' suite of S-type granites. The mid-Ordovician middle crust of NE Scotland was thus a site of crustal differentiation. The results demonstrate that crustal fusion and magma production can occur without significant chemical interaction between the mantle-derived heat source and the crustal melts, and that melt extraction can occur in the absence of regional tectonic deformation.

KEY WORDS: *migmatite; diatexite; fluid-absent melting; melt segregation; peraluminous granite*

INTRODUCTION

The differentiation of the continental crust is widely held to involve the partial melting of mid- to deep-crustal rocks, at high metamorphic grades, with the upward escape of granitic melts, leaving behind high-grade restitic residues (Clemens, 1990; Thompson, 1990; Vielzeuf *et al*., 1990). Intracrustal heat sources are generally inadequate to power these processes, and major contributions of mantle heat seem to be required (England & Thompson, 1986). Such mantle-derived heat is most easily supplied through intrusion of gabbroic magmas into the crust. Exposed examples of contact anatexis surrounding gabbroic intrusions are therefore of considerable interest. This paper describes a particularly instructive example of this, and explores the nature of the petrogenetic processes involved.

Partial melting phenomena are commonly recognized in the inner parts of the thermal aureoles of large mid- and upper-crustal intrusions, where the wall rocks are of suitable composition (e.g. Ashworth & Chinner, 1978; Pattison & Harte, 1988; Grant & Frost, 1990; Finger & Clemens, 1995; Holness & Clemens, 1999). In the context of crustal differentiation, a key question is the extent to which the anatectic melts migrate away from, or remain within, their sites of generation in such aureoles. In principle, several potential fates can be envisaged for contact-anatectic melts; they can (1) crystallize *in situ* (e.g. Pattison & Harte, 1988); (2) intrude the chilled margin of the pluton, forming back-veining complexes; (3) invade the magma of the pluton, either to mix with it (if miscible) to produce a hybrid magma (e.g. Greenfield *et al*., 1996) or mingle with it (if immiscible or inefficiently comminuted) to form enclaves; (4) migrate elsewhere in the inner aureole, either by flowing along fractures or by percolating along grain-boundaries; (5) leave the aureole to intrude cooler country rock at higher crustal levels. *In situ* crystallization is most likely to occur where the heat-supplying pluton is at relatively low temperature (i.e. a granitoid magma) and generally produces relatively small volumes of anatectic melt by fluid-saturated reactions (e.g. Holness & Clemens, 1999). Such reactions tend to have negative dP/dT slopes, causing near-solidus fluid-saturated melts to solidify immediately if they begin to ascend (Brown & Fyfe, 1970). Conversely, melts are likely to be able to leave the aureole to intrude cooler country rocks only if the heat-supplying pluton is relatively large, hot (i.e. mafic) and produces relatively large volumes of low-viscosity, fluid-undersaturated anatectic melt, by fluid-absent reactions. Such reactions have positive dP/dT slopes, allowing the melts to ascend for appreciable distances without immediately freezing (Brown & Fyfe, 1970; Clemens *et al*., 1997; Clemens & Droop, 1998).

If it occurs on a large enough scale, the segregation and ascent of anatectic melt from its source region must result in crustal differentiation, with enrichment of the source areas in refractory (restitic) components, and of higher crustal levels in the complementary 'granitophile' components. It has been suggested that the intraplating and underplating of the crust by large volumes of mafic magma and the ensuing partial melting of fertile crustal rocks is the major process by which mobile granitoid magmas are produced and the continental crust grows in volume (e.g. Clemens, 1990; Rudnick, 1990; Vielzeuf *et al*., 1990; Stevens & Clemens, 1993). In a deep-crustal context, petrological and geochemical evidence for granitic melt extraction and restite formation is well documented (e.g. the granulite-facies 'stronalites' of the Ivrea Zone, northern Italy; Schnetger, 1994). However, so far, there has been little to suggest that these processes could also operate at mid-crustal levels. In this paper, we examine the thermal effects of a large gabbro intrusion and present evidence that it caused substantial restite formation, at mid-crustal levels. We demonstrate that the country-rock metapelites underwent very high degrees of partial melting and that, locally, a large proportion of the melts segregated from the solid residua, and indeed escaped the source region.

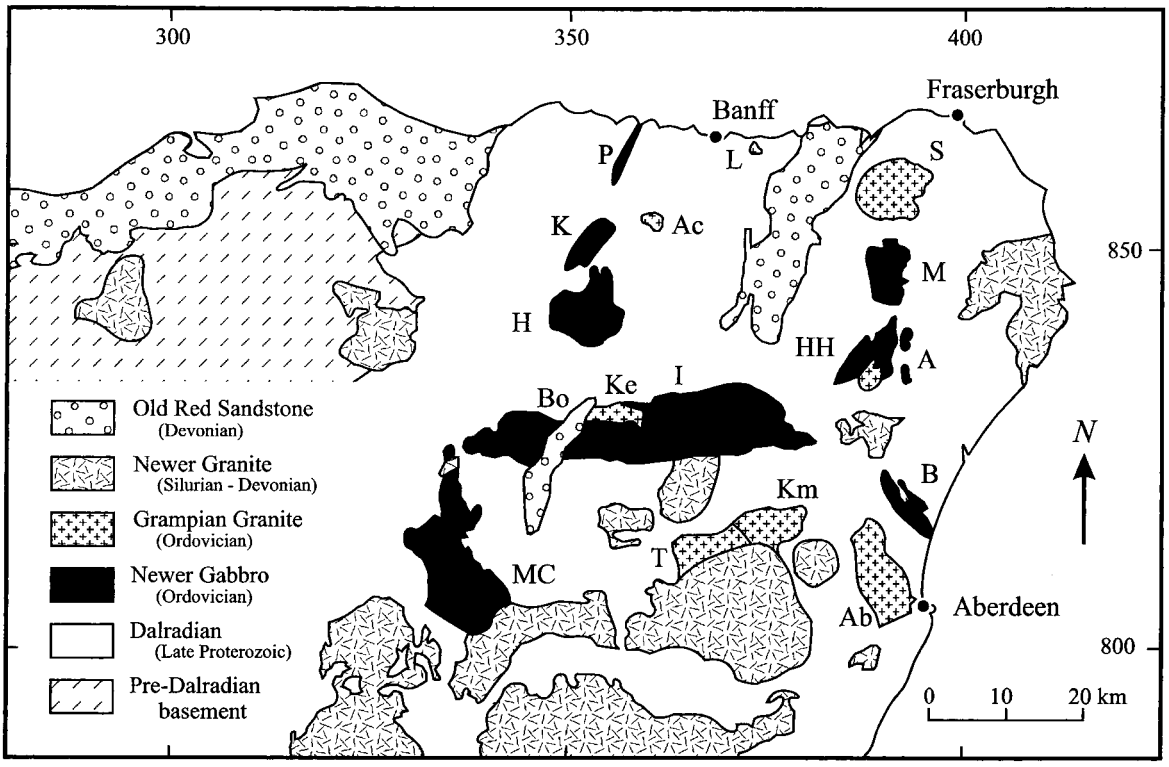

Fig. 1. Sketch map of the geology of NE Scotland. Coordinates: Ordnance Survey, British National Grid. Newer Gabbros: A, Arnage; B, Belhelvie; Bo, Boganclogh; H, Huntly; HH, Haddo House; I, Insch; K, Knock; M, Maud; MC, Morven–Cabrach; P, Portsoy. Grampian Granites: Ab, Aberdeen; Ac, Aberchirder; Ke, Kennethmont; Km, Kemnay; L, Longmanhill; S, Strichen; T, Tillylourie.

GEOLOGICAL SETTING

The Huntly Gabbro in NE Scotland (Fig. 1) is one of a suite of large, syn-orogenic, layered, mafic intrusions of Middle Ordovician age, locally known as the 'Newer Gabbros' (Read, 1919, 1923, 1961). These were emplaced into Dalradian (Late Proterozoic) metaclastic rocks during, or soon after, the thermal peak of the Grampian regional metamorphism (Fettes, 1970).

The classic Buchan-type regional metamorphism in NE Scotland is characterized by a sequence of biotite, cordierite, andalusite and sillimanite zones in the metapelites (Read, 1923*a*, 1952). The metamorphism occurred statically under conditions of high temperature and low pressure (Chinner, 1966; Harte & Hudson, 1979; Hudson, 1980, 1985). The regional isograds describe a broad horseshoe pattern around a central area of low-grade rocks (Read, 1952), probably as a result of post-metamorphic folding (Treagus & Roberts, 1981).

The Newer Gabbro intrusions themselves display rhythmic and cryptic layering, and consist mainly of cumulate-textured peridotites (now serpentinized), troctolites, norites, gabbros and, locally, more differentiated monzogabbros (Wadsworth *et al.*, 1966; Clarke & Wadsworth, 1970; Ashcroft & Boyd, 1976; Wadsworth, 1982, 1986, 1988; Munro, 1984). The gabbros post-date at least one phase of regional ductile deformation in the Dalradian country rocks, but were themselves affected by post-magmatic shearing, particularly along their contacts (Ashcroft & Munro, 1978; Boyd & Munro, 1978; Ashcroft *et al.*, 1984). Stewart & Johnson (1960) suggested that the various gabbro bodies represent the dismembered remains of a single lopolith. However, as the details of the modal layering differ from one body to another (Munro, 1984), it is more likely that the intrusions evolved independently by *in situ* crystal fractionation of separate magma batches (Wadsworth, 1986). Pankhurst (1970) obtained a whole-rock Rb–Sr isochron date of 486 ± 17 Ma for the Newer Gabbros, but more precise U–Pb mineral ages of 468 ± 8 Ma and 470 ± 9 Ma have been obtained by Rogers *et al.* (1994) and Dempster *et al.* (2002), respectively.

Many of the Newer Gabbros possess well-developed thermal aureoles (e.g. Stewart, 1946; Gribble, 1966; Allan, 1970; Fettes, 1970; Ashworth, 1975), some of which have locally modified the regional isograd pattern (e.g. Fettes, 1970). Thus, rather than having been

entirely responsible for it, the exposed gabbro bodies appear to have locally augmented the regional metamorphism (Pankhurst, 1970). This seems to be a common feature of plutonometamorphism (Powers & Bohlen, 1985; Wickham, 1987; Finger & Clemens, 1995). Pressure estimates of ~0·4–0·5 GPa from the thermal aureoles (Ashworth & Chinner, 1978; Droop & Charnley, 1985) indicate that the Newer Gabbros were emplaced at a depth of ~15–18 km. The pressure increase recorded by the overprinting of andalusite by kyanite in schists structurally beneath the gabbros (Chinner & Heseltine, 1979; Chinner, 1980) has been attributed to the extra load imposed by the intrusions (Dempster *et al*., 1995) or to post-intrusive thrusting (Baker, 1987).

Outcrops of xenolithic rocks (diatexitic schollen migmatites), composed of a cordierite-bearing igneous matrix and xenoliths of silica-poor aluminous hornfels, are closely associated with several of the Newer Gabbros, both in their inner aureoles and within the gabbros themselves. Watt (1914) and Read (1923*a*, 1923*b*, 1935), who first described these xenolithic complexes, believed that the igneous matrix rocks, which they termed 'cordierite norites', had been produced by contamination of mafic magma by assimilation of pelitic wall rocks. Chinner & Schairer (1962), Gribble & O'Hara (1967) and Gribble (1968, 1970) later demonstrated that formation of cordierite norites by bulk assimilation of metapelite by mafic magma could not occur by a process of down-temperature evolution, owing to the existence of the An–Opx–Tri thermal divide in the CMAS system. Instead, they argued that the 'cordierite norites' were derived by partial melting of Dalradian metapelites, without significant mixing with the Newer Gabbro magmas, a view supported by their relatively high $^{87}Sr/^{86}Sr$ initial ratios (0·720–0·730; Pankhurst, 1969).

Granitoid plutons are volumetrically abundant in NE Scotland (Fig. 1). Of these, the 'Grampian Granites' (Brown, 1991) are late-tectonic peraluminous granites of Ordovician age (Pankhurst, 1974), which have yielded U–Pb mineral ages of 475 ± 5 Ma (Pidgeon & Aftalion, 1978), 470 ± 1 Ma (Kneller & Aftalion, 1987) and 467 ± 6 Ma (Oliver *et al*., 2000). The coincidence between these ages and those of the Newer Gabbros indicates that there was a major thermal event in the Buchan area at that time, involving high-T, low-P regional metamorphism, gabbro intrusion, crustal melting and the generation of granite magmas (Rogers *et al*., 1994).

THE HUNTLY COMPLEX

The Huntly Complex is a poorly exposed, pear-shaped outcrop of gabbros and associated rocks, measuring ~10 km × 9 km, intruding broadly north–south-trending Dalradian metasediments of the Argyll and Southern Highland Groups (Fig. 2). The southern contact cuts andalusite-porphyroblastic metapelites of the Boyndie Bay Group and turbiditic metapelites and psammites of the Whitehills Group. The western contact abuts biotite-rich garnet-, staurolite- and sillimanite-bearing schists and gneisses of the Portsoy Group. The mafic igneous rocks crop out in two major areas, one to the west, comprising mainly layered cumulate troctolites, and one in the east–central part, comprising mainly gabbronorites and norites (Munro, 1970; Weedon, 1970). The cumulate layering dips steeply and youngs to the east (Shackleton, 1948), indicating that the western margin of the complex was the original floor of the intrusion. The thermal aureole surrounding the Huntly Complex has not been mapped. This is due partly to the general paucity of exposure and partly (at least around the western margin) to excision of the aureole by faulting (Munro, 1970) along a NNE-trending zone of intense strain (Baker, 1987) known as the 'Portsoy–Duchray Lineament' (Harte, 1988). However, closely associated with the mafic igneous rocks are numerous outcrops of migmatite ('xenolithic complexes') (Fig. 2), which undoubtedly represent high-grade contact metamorphic rocks. Many of these appear to be arranged around the margins of the complex, particularly on the eastern side, but isolated outcrops of migmatite also occur within the gabbros (Fig. 2) (Munro, 1970). Judging by the trends in strike of the country rock units, it is likely that the migmatites in the southern part of the complex (Huntly–Dunbennan Hill) were derived from schists of the Boyndie Bay and Whitehills Groups. Two kilometre-scale granites also occupy marginal positions in the complex (Fig. 2). The more northerly of these granites (Avochie) is foliated (Munro, 1970) and may belong to the Grampian suite.

PETROGRAPHY OF METAPELITES

In this section we describe the field relations, mineralogy and textures of pelitic country rocks and migmatites from the southern and western parts of the Huntly Complex. Mineral assemblages of representative samples are listed in Table 1.

Regional metamorphic rocks

The regional metamorphic rocks exposed around the south and west margins of the Huntly Complex span a wide range in mineralogy, texture and grade. Biotite-slates of the lowermost Macduff Slate crop out at St. Michael's Well (British National Grid reference NJ 519359) and Coynachie (NJ 491344), south of the area covered by Fig. 2. These rocks are fine-grained

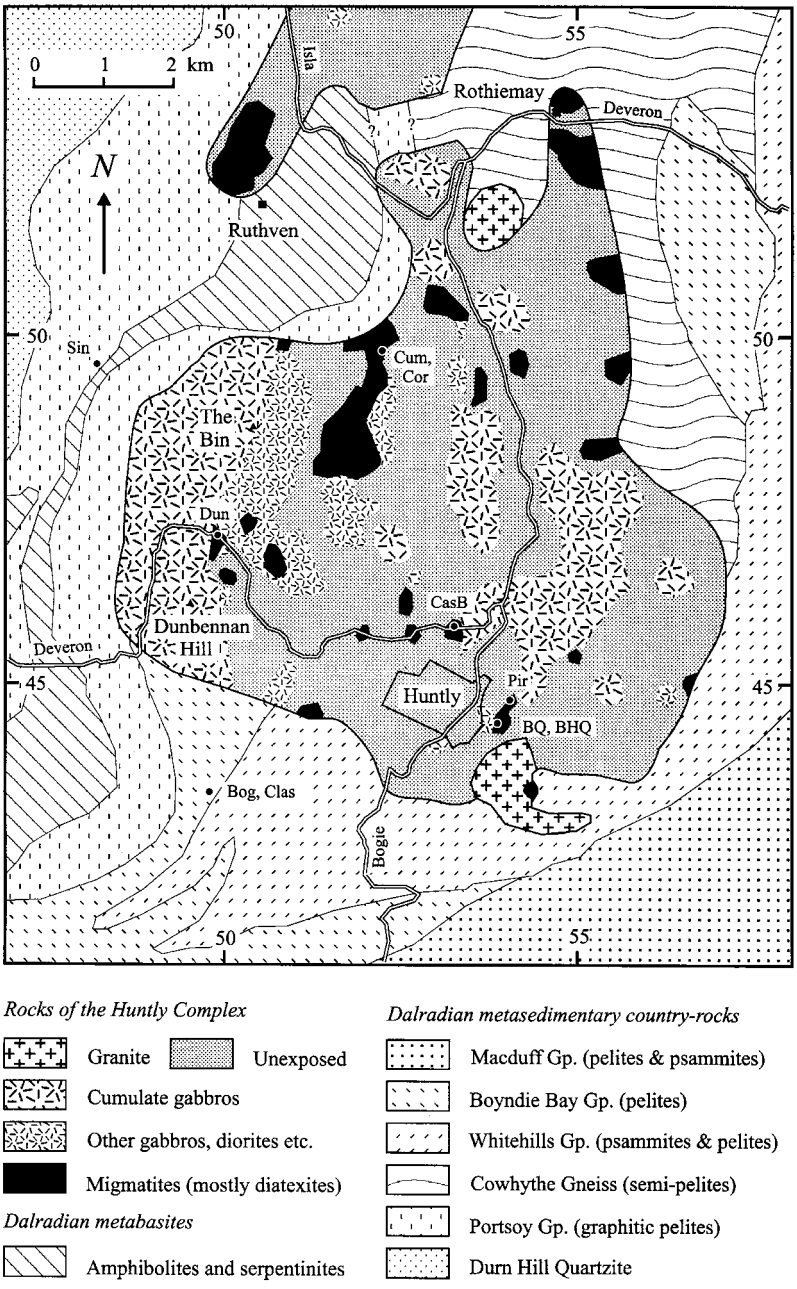

Fig. 2. Geological map of the Huntly Gabbro and associated rocks, showing localities of key sample sets (dots: identified by field-number prefix: BQ, BHQ, Battlehill Quarry; Pir, north side of Battlehill; CasB, Castle Bridge; Dun, Dunbennan Wood; Cum, Cor, Cumrie–Cormalet; Sin, Cairnie road cutting; Bog, Clas, Clashmach Hill). Rock types within the Huntly Complex from Munro (1970); outcrops (approximate) of Dalradian units from Geological Survey of Scotland, Sheet 86. Coordinates: OS British National Grid, square NJ.

cleaved metasiltstones with millimetre- to centimetre-scale compositional layering (bedding) defined by alternating quartz-rich and quartz-poor layers, and an oblique penetrative cleavage defined by aligned biotite, muscovite and chlorite flakes. The rocks belong to the Buchan biotite zone.

Coarser-grained pelitic mica schists and subordinate semipelites (metagreywackes) and quartzites of the Boyndie Bay Group occur further west, in the vicinity of Clashmach Hill (NJ 498385). The schists contain the assemblage Ms + Bt + Qtz + Pl ± And ± St ± Grt + Ilm. Aligned muscovite flakes measuring ~500 μm × 50 μm

Table 1: Mineral assemblages of representative metasedimentary rocks from the southern and western parts of the Huntly complex

Regionally metamorphosed metapelitic schists				
Sin1	Garnet–biotite gneiss	482446	Grt + Sil + Bt + Qtz + Pl (+ Zrn + Ilm)	{10}
Sin2	Garnet–mica schist	482446	Grt + Bt + Ms + Qtz + Pl (+ Ilm + Ap + Zrn)	{19}
Sin101	Garnet–biotite gneiss	482446	Grt + St + Bt + Qtz + Pl (+ Zrn + Chl^R)	{20}
Bog1	Mica schist	498385	Bt + Ms + Qtz + Pl (+ Tur + Ilm)	{8}
Bog3	And–mica schist	498385	And + Bt + Ms + Qtz + Pl (+ Tur + Ilm)	{10}
Clas66	And–mica schist	498385	And + Bt + Ms + Qtz + Pl (+ Grt + St + Tur + Ilm)	{16}
Clas112	And–mica schist	498385	And + Bt + Ms + Qtz + Pl (+ Grt + St + Tur + Ilm)	{11}
Mike1	Biotite slate	519359	Bt + Chl + Ms + Qtz (+ Ilm)	
Metapelitic hornfelses (including melanosomes in metatexites and xenoliths in diatexites)				
Cor2	Crd–Kfs hornfels	523448	Grt + Crd + Bt + Qtz + Kfs + Pl + Sil^R (+ Ilm + Zrn)	
Cor6	Crd–Kfs hornfels	523448	Grt + Crd + Hc + Bt + Kfs + Pl + Sil^R (+ Ms^R + Ilm + Zrn)	
Cor11a	Crd–Kfs hornfels	523448	Crd + Kfs + Pl (+ Hc + Bt + Ilm + Zrn)	
Cor8	Crd–Kfs hornfels	523448	Grt + Crd + Sil^R + Bt + Kfs + Pl (+ Qtz + Hc + Ilm + Zrn)	
Dun1	Sil–Crd hornfels	499422	Grt + Sil + Crd + Bt + Qtz + Pl (+ And^R + Chl^R + Ilm + Zrn + Gr)	
Cor10a	Opx–Crd hornfels	523448	Grt + Opx + Crd + Bt + Kfs + Pl + Ilm (+ Hc^I + Qtz + Zrn)	
BHQ5	Opx–Crd hornfels	539395	Grt + Opx + Crd + Hc + Pl + Ilm (+ Zrn)	
9994	Opx–Crd hornfels	539395	Opx + Crd + Hc + Kfs + Pl + Ilm (+ Bt^R)	
9996a	Opx–Crd hornfels	539395	Grt + Opx + Crd + Kfs + Pl + Ilm (+ Zrn)	
10035	Opx–Crd hornfels	539395	Grt + Opx + Crd + Hc + Pl + Ilm (+ Bt + Zrn)	
BQ17	Opx–Crd hornfels	539395	Grt + Opx + Crd + Hc + Kfs + Pl + Ilm (+ Bt + Zrn)	
BQ41	Opx–Crd hornfels	539395	Grt + Opx + Crd + Fsp + Ilm (+ Bt + Zrn)	
Pir1	Opx–Crd hornfels	541398	Grt + Opx + Crd + Hc + Kfs + Pl + Ilm (+ Bt^R)	
Igneous-textured metapelitic rocks (including leucosomes in metatexites and matrices of diatexites)				
Cor11b	Leucosome	523448	Grt + Kfs + Pl + Qtz (+ Crd + Bt + Ilm + Zrn)	
9996b	Leucosome	539395	Crd + Kfs (+ Grt + Hc^I + Qtz + Pl + Ilm)	
Cum22	Grt tonalite	523448	Grt + Bt + Qtz + Pl + Kfs (+ Ilm + Ap + Zrn)	
Cor7	Grt–Crd tonalite	523448	Grt + Crd + Bt + Qtz + Pl (+ Sil + Ms^R + Ilm + Ap + Zrn + Mnz)	
Fow1	Grt–Crd tonalite	532528	Grt + Crd + Hc + Bt + Pl + Kfs (+ Qtz + Sil^P + Ilm + Zrn)	
BHQ1	Cordierite norite	539395	Grt + Opx + Crd + Bt + Qtz + Pl + Kfs (+ Hc^I + Ilm + Zrn)	
BQ38	Cordierite norite	539395	Grt + Opx + Crd + Bt + Qtz + Pl (+ Hc° + Ilm + Zrn)	
BQ202	Cordierite norite	539395	Grt + Opx + Crd + Bt + Qtz + Pl (+ Kfs + Hc° + Ilm + Zrn + Mnz)	
Dun4	Cordierite norite	499422	Grt + Opx + Crd + Hc^I + Bt + Qtz + Pl (+ Sil^P + Ath^R + Ilm + Zrn + Gr)	
Dun10	Cordierite norite	499422	Grt + Opx + Crd + Hc^I + Bt + Qtz + Kfs + Pl (+ Ilm + Zrn + Gr)	
Dun12	Cordierite norite	499422	Grt + Opx + Crd + Hc^I + Bt + Pl (+ Qtz + Ath^R + Ilm + Zrn + Gr)	
CasB2i	Cordierite norite	533409	Grt + Opx + Crd + Hc^I + Bt + Qtz + Pl (+ Sil^P + Ilm + Zrn)	
CasB5	Cordierite norite	533409	Grt + Opx + Crd + Hc^I + Bt + Qtz + Pl (+ Ilm + Zrn + Gr)	

Mineral name abbreviations from Kretz (1983); Fsp, anorthoclase. Grid references are for OS BNG square NJ. R, retrograde mineral; P, relict prograde mineral; I, only as inclusions within, or intergrowths with, cordierite; O, only as inclusions within Crd, Grt, Opx and Pl. Modally minor phases shown in parentheses. Numbers in curly brackets are estimated modal percentages of plagioclase.

define the schistosity, whereas more equant, randomly orientated biotite flakes and granoblastic quartz and plagioclase make up the rest of the matrix. Andalusite occurs as sub-rectangular poikiloblasts, up to 6 mm long, containing quartz inclusions. Staurolite forms subhedral micropoikiloblasts up to 0·3 mm long. Rare, tiny (~150 μm diameter) subhedral garnets occur in some samples. These rocks belong to the

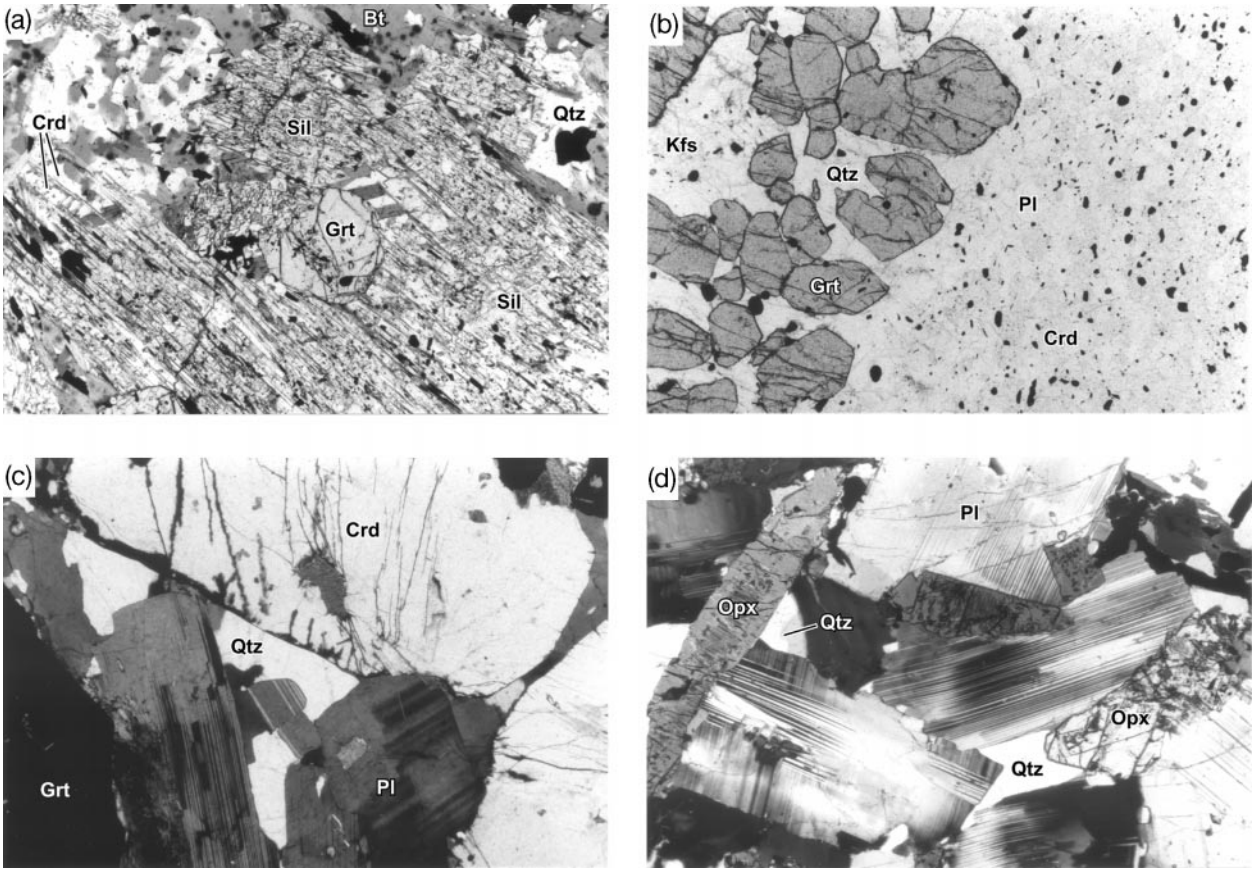

Fig. 3. Photomicrographs of textural features in pelites associated with the Huntly Complex. Field of view 4·2 mm × 2·8 mm. (a) Sillimanite–granofels sample Dun1, showing garnet (Grt) and large clusters of sillimanite prisms (Sil) in a fine-grained matrix of biotite (Bt), cordierite (Crd) and quartz (Qtz). Plane-polarized light. The sillimanite clusters are interpreted as pseudomorphs after andalusite. (b) Metatexite sample Cor11, showing textural and mineralogical contrast between fine-grained melanosome (to right), composed of cordierite (Crd), plagioclase (Pl) and ilmenite (opaque), and coarse-grained leucosome (to left) composed of subhedral garnet (Grt) and interstitial K-feldspar (Kfs) and quartz (Qtz). Plane-polarized light. (c) Igneous-textured garnet–cordierite tonalite sample Cor7, showing large, euhedral, relatively inclusion-free crystals of garnet (Grt), cordierite (Crd) and plagioclase (Pl) and cuspate interstitial patches of quartz (Qtz). Crossed polars. (d) Igneous-textured garnet–cordierite norite sample BQ38, showing large, euhedral crystals of orthopyroxene (Opx) and plagioclase (Pl) and cuspate interstitial patches of quartz (Qtz). Crossed polars.

Buchan upper andalusite zone [the staurolite zone of Hudson (1980)].

West of the Huntly Complex, rocks of the Portsoy Group were sampled at Cairnie (NJ 482446). Many samples (e.g. Sin1, Sin101) are medium-grained plagioclase- and quartz-rich garnet–biotite gneisses containing minor staurolite or fibrolitic sillimanite. The rocks possess a biotite ± sillimanite schistosity, parallel to a layering defined by variations in modal biotite proportion. Somewhat finer-grained garnet–mica schists (e.g. Sin2) lack modal layering and contain essential muscovite, which, together with biotite, defines the schistosity. The garnets form anhedral inclusion-free crystals up to 0·4 mm across. These schists and gneisses, which belong to the lower sillimanite zone, appear to belong to a facies series of Barrovian (medium P/T) type.

Non-migmatitic hornfels

A loose block (>1 m diameter) of non-migmatitic cordierite–sillimanite hornfels (Dun1), representing a contact-metamorphosed metapelite that did not undergo partial melting, was found on the eastern side of the River Deveron (NJ 499422) near Dunbennan Hill in the SW part of the complex. The rock contains scattered subhedral garnet porphyroblasts up to 3 mm across and abundant large (~8 mm × 2 mm × 2 mm) randomly orientated bundles of sub-parallel prismatic sillimanite crystals, set in a fine-grained granoblastic matrix of biotite, cordierite, plagioclase, quartz and ilmenite (Fig. 3a). Cordierite is locally replaced by retrograde chlorite + andalusite. The sillimanite aggregates are elongated and roughly square in cross-section, suggesting that they are pseudomorphs after

andalusite. Similar sillimanite pseudomorphs after andalusite have been described by Vernon (1987).

Migmatites

The majority of contact-metamorphic rocks in the Huntly Complex are migmatites, and those described below correspond mainly to the 'cordierite-bearing migmatites' of Ashworth (1976). The following descriptions, although overlapping in part with those of Ashworth (1976), concentrate on new observations. Migmatite terminology used in this paper is from Ashworth (1985).

Metatexites

Large loose blocks of stromatic metatexite are abundant in the vicinity of Cumrie and Cormalet Hill in the north central part of the Complex (Fig. 2). These rocks typically consist of blue–grey cordierite hornfels melanosomes and veins of garnetiferous leucosome, the latter typically occupying ~20–40% of the rock. The hornfels melanosomes are fine grained and locally contain garnet porphyroblasts. The leucosomes are mostly <1 cm thick and tend to form sub-parallel arrays, following the primary lithological layering (bedding), even where the latter is tightly folded. In most metatexites, however, branching, anastomosing and crosscutting veins also occur, indicating the former presence of a melt phase. Leucosome veins have locally coalesced to form irregular granitic patches (>5 cm across), studded with large garnets.

Most melanosomes are Opx-free Crd–Kfs hornfelses (e.g. Cor2, Cor6 and Cor11a; Table 1). Cordierite, plagioclase, K-feldspar and ilmenite all occur as equant, anhedral grains and form a typical granoblastic polygonal matrix (Fig. 3b). Randomly orientated, thin, red–brown biotite flakes are partially replaced by fibrolitic sillimanite in some rocks. Quartz, where present, is usually subordinate, interstitial and texturally associated with garnet. In some quartz-free hornfelses, small granules of brown hercynite occur in the matrix. The K-feldspar is commonly microperthitic and locally replaced by myrmekitic quartz–plagioclase intergrowths. Garnet, where present, typically forms euhedral porphyroblasts, up to 5 mm in diameter, containing rounded inclusions of ilmenite, biotite and, in some rocks, hercynite, near its rims. In some hornfelses, however, the garnets have atoll-like or spongy textures and are intergrown with relatively coarse-grained quartz and K-feldspar. Apart from the fact that they appear to be isolated and spheroidal, rather than planar, these quartz–K-feldspar–garnet aggregates closely resemble the leucosomes described by Powell & Downes (1990) from pelitic granulites at Broken Hill and, like them, probably represent localized sites of melting.

The leucosomes are dominated by quartz, K-feldspar and garnet with subordinate biotite, plagioclase and cordierite (e.g. Cor11b: Table 1). The garnet is typically inclusion free, and forms either irregular grains (Fig. 3b) or large (up to 1 cm diameter) euhedral crystals. The K-feldspar forms blocky, subhedral crystals of coarse-grained orthoclase microperthite, to which quartz is locally interstitial.

Garnet is a common solid product of incongruent, biotite-consuming, fluid-absent melting reactions in aluminous rocks (Waters & Whales, 1984; Grant, 1985*a*, 1985*b*; Conrad *et al.*, 1988; LeBreton & Thompson, 1988; Vielzeuf & Holloway, 1988; Waters, 1988; Powell & Downes, 1990; Vielzeuf & Montel, 1994; Carrington & Harley, 1995; Patiño Douce & Beard, 1996; Stevens *et al.*, 1997; Pickering & Johnston, 1998). The ubiquity and abundance of garnets in the leucosomes provides strong evidence that this type of reaction was responsible, at least in part, for the migmatization of the Huntly rocks.

Diatexite matrices (Grt tonalites and Crd norites)

Schollen diatexites are common throughout the Huntly Complex (Fig. 2). On a mesoscopic scale, these rocks typically consist of ~70–95% of medium- to coarse-grained, igneous textured mobilisate ('matrix') with subordinate irregular hornfels or metatexite schollen up to 1 m long. Most of the schollen are pelitic, but other refractory rock types, such as quartzite and calc-silicate, occur locally.

The diatexite matrix rocks have pelitic or semi-pelitic mineralogies but igneous textures. Opx-free varieties ['granitoids' of Ashworth (1976)] are well represented in the Cormalet–Cumrie area. The Grt tonalite sample Cor7 (Table 1; Fig. 3c), for example, consists of abundant large (~1 cm diameter) euhedral, inclusion-free garnets and sporadic, blocky, euhedral, inclusion-free cordierites in a medium- to coarse-grained matrix of biotite, quartz and euhedral plagioclase. Much of the quartz is clearly interstitial to garnet, cordierite and plagioclase (Fig. 3c). Small patches of fibrolite occur locally, near the cordierite and garnet.

Opx-bearing varieties ['cordierite norites' of Read (1923, 1935); 'noritoids' of Ashworth (1976)] crop out within the complex at Battlehill Quarry (NJ 539395), and in the River Deveron at Castle Bridge (NJ 533409) and north of Dunbennan Hill (NJ 499422) (Fig. 2). At Battlehill Quarry, such rocks form discordant bodies with sharp contacts against biotite–hornblende gabbro, micronorite and Opx–Crd hornfels. They are typically medium-grained

rocks of mafic igneous appearance, rich in prominent, randomly orientated crystals of cordierite, orthopyroxene, garnet and plagioclase. The cordierite is fresh and forms subhedral prismatic crystals with well-developed simple or sector twinning. The orthopyroxene is markedly pleochroic and typically forms elongated subhedral prisms (Fig. 3d), locally enclosing rounded plagioclase inclusions. Garnet, commonly less abundant than Opx and Crd, forms subhedral grains that are either inclusion free or contain scattered ilmenite and biotite inclusions. Plagioclase crystals are subhedral and commonly show normal zoning, with sharply demarcated cores and rims, and locally also oscillatory zoning. In samples from Castle Bridge (e.g. CB1) biotite forms thick, subhedral books up to 1·5 mm across, but in others it appears to be mainly interstitial. In sample BHQ1 it forms large poikilitic patches, up to 8 mm across, enclosing plagioclase and cordierite. Quartz is generally present only in minor amounts and commonly forms small cuspate grains interstitial to garnet, cordierite, orthopyroxene and plagioclase (Fig. 3d). These quartz grains texturally resemble the 'melt pools' figured by Sawyer (2001). Samples from Castle Bridge contain modally abundant quartz, in part clearly interstitial to the ferromagnesian minerals. K-feldspar (orthoclase microperthite) is present in only a few cordierite norites and is generally poikilitic or interstitial to plagioclase and ferromagnesian minerals. Dark green hercynite is a constituent of many Crd norites. In samples from Battlehill Quarry hercynite is a minor phase and tends to occur only as small inclusions within cordierite, although in some samples (e.g. BQ38, BQ202) it is also enclosed by orthopyroxene, plagioclase and garnet. Hercynite is modally abundant in many Crd norites from Castle Bridge and Dunbennan Hill, where it forms oblong clusters, measuring up to 5 mm × 2 mm × 2 mm, of 0·01–0·1 mm granules intergrown with fine-grained cordierite. These hercynite clusters locally have square cross-sections and, in one sample (Dun4), are locally cored by corroded aggregates of prismatic sillimanite (Fig. 4a), indicating that they are pseudomorphs after that mineral. This texture also occurs in Crd-rich Grt tonalite sample Fow1. Hercynite has not been found in contact with quartz in any Huntly diatexite matrix rock. Retrograde textures include symplectic intergrowths of biotite and quartz replacing orthopyroxene and fine-grained biotite rimming garnet (Ashworth, 1976).

The igneous textures of the diatexite mobilisates clearly indicate that they contained a melt phase during crystallization (see also Kenah & Hollister, 1983; Vernon & Collins, 1988; Harte *et al.*, 1991). These rocks resemble cumulates in that the abundant, large, subhedral to euhedral cordierites, orthopyroxenes, garnets and plagioclase cores clearly crystallized early, whereas the plagioclase rims and the modally minor, interstitial or poikilitic quartz, K-feldspar and biotite clearly crystallized later. The question arises as to whether the large crystals precipitated from the melt as phenocrysts or represent the solid products of incongruent melting reactions. We favour the latter interpretation because (1) the temperatures required to completely melt aluminous metapelites are higher, and presumably therefore less readily attained, than those necessary for partial melting, (2) cordierite, garnet and orthopyroxene are known to form during incongruent melting of biotite (e.g. Grant, 1985*a*, 1985*b*), and (3) the Opx–Crd hornfelses (see below) contain similar assemblages to some of the cordierite norites but have textures indicative of solid-state equilibration.

Crd–Kfs hornfels schollen

Crd–Kfs hornfels schollen (e.g. Cor8) within garnet granitoids at Cormalet closely resemble hornfels melanosomes in metatexites, both texturally and mineralogically.

Opx–Crd hornfels schollen and xenoliths

Opx–Crd hornfelses occur in the southern and western parts of the Huntly Complex as schollen within 'cordierite norites' and as screens in gabbroic rocks. At Battlehill Quarry, sharp contacts are exposed between biotite–hornblende gabbro and screens of Opx–Crd hornfels up to 6 m thick. The attitude of the lithological layering varies dramatically from one screen to the next, indicating that the screens are large xenoliths. A 3 m thick xenolith of Opx–Crd hornfels is in sharp contact with biotite gabbro in a small quarry on the NW side of Battlehill Woods (NJ 511398).

The hornfelses are fine-grained, layered, dark bluish grey cordierite-rich rocks, commonly bearing small (1–2 mm) garnet porphyroblasts. The matrices typically consist mainly of small equant grains of orthopyroxene, plagioclase and twinned cordierite, accompanied by abundant granules of ilmenite and, in many samples, dark green hercynite. The grains have random orientations and a well-developed granoblastic polygonal texture (Fig. 4b), indicating a high degree of textural equilibration. Plagioclase is only rarely zoned. Cordierite tends to have a slightly larger grain size than Opx and Pl and locally forms subhedral porphyroblasts. Plagioclase is absent from samples BQ41 and BQ101, but its place is taken by anorthoclase. Some samples (e.g. BQ17) contain sporadic 2 mm × 1 mm composite plagioclase–K-feldspar intergrowths, which may be exsolved ternary feldspars. Quartz is usually absent. Garnet occurs mainly as

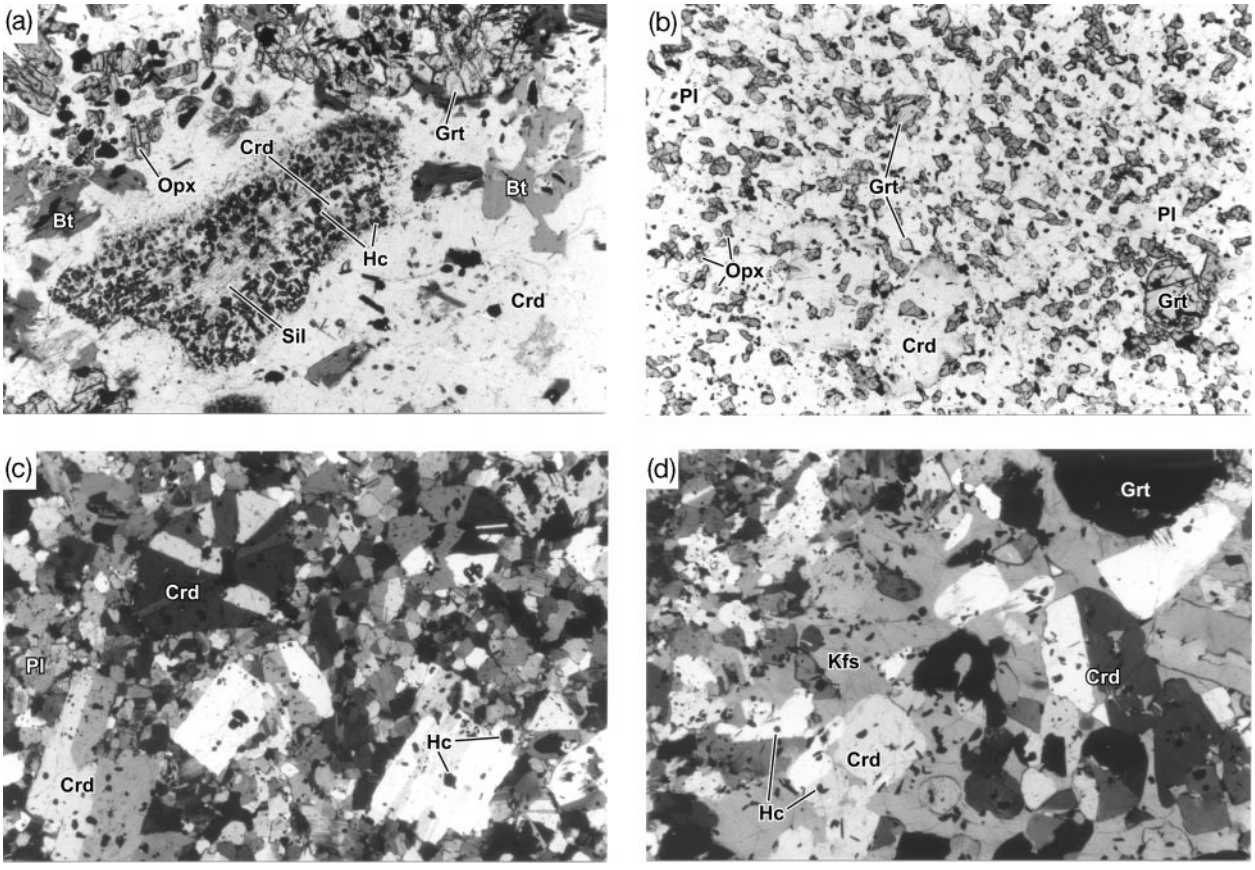

Fig. 4. Photomicrographs of textural features of pelites associated with the Huntly Complex. Field of view 4·2 mm × 2·8 mm. (a) Garnet–cordierite norite sample Dun4, showing microgranular corona of hercynite (He) and cordierite (Crd) surrounding relict sillimanite (Sil) in a medium-grained, igneous-textured matrix of garnet (Grt), orthopyroxene (Opx), biotite (Bt) and cordierite (Crd). Plane-polarized light. (b) Cordierite–orthopyroxene hornfels sample BQ17, showing porphyroblasts of garnet (Grt) and cordierite (Crd) in a fine-grained, granoblastic matrix of orthopyroxene (Opx), plagioclase (Pl) and ilmenite (opaque) with rare tiny, euhedral garnet grains. Plane-polarized light. (c) Cordieritite sample 10035, showing subhedral to euhedral, twinned porphyroblasts of cordierite (Crd) in a fine-grained, granoblastic matrix of cordierite, plagioclase (Pl) and hercynite (Hc). Crossed polars. (d) Leucosome vein in cordieritite sample 9996. The leucosome (on the right) is medium to coarse grained and consists of subhedral crystals of garnet (Grt) and cordierite (Crd) and granules of hercynite (Hc) poikilitically enclosed by K-feldspar (Kfs). The fine-grained granoblastic cordieritite is visible on the upper left. Crossed polars.

subhedral porphyroblasts (Fig. 4b), locally with inclusions of ilmenite and hercynite but, in some samples, also forms tiny euhedral crystals (Fig. 4b) and anhedral rims around ilmenite grains. Hercynite is in contact with cordierite, garnet, orthopyroxene and plagioclase but not quartz. Biotite is rare or absent.

Some hornfelses (e.g. HBHQ5, 9996, 10035, BW202) contain exceptionally high modal amounts of cordierite (>60%), with subordinate plagioclase, orthopyroxene, garnet, ilmenite and hercynite (Fig. 4c), and are referred to here as 'cordieritites'.

Many Opx–Crd hornfelses possess compositional layering, manifest as variations in both modal mineralogy and mean grain size. Relatively coarse-grained layers tend to be more leucocratic than the finer-grained layers; they lack hercynite, and contain appreciable amounts of interstitial K-feldspar, quartz and biotite. Garnets in such layers are either irregular porphyroblasts or atoll-type grains filled with relatively coarse biotite, K-feldspar and quartz. These layers have textures reminiscent of the leucosomes in the metatexites, but are less clearly demarcated from melanosomes. Distinct leucosomes do, however, exist. A 6 mm thick vein of medium-grained Grt–Crd–Kfs rock cuts the cordieritite of sample 9996. This igneous-textured leucosome consists of abundant, euhedral to subhedral, twinned cordierites (with inclusions of ilmenite and hercynite) and rare garnets enclosed by coarse poikilitic K-feldspar (Fig. 4d). In many respects this rock resembles the diatexite matrix rocks described above.

Disregarding interstitial, leucosome and poikilitic minerals, the characteristic peak-metamorphic mineral assemblage of the majority of Opx–Crd hornfelses is Crd + Opx + Grt + Hc + Pl + Ilm. Fine-grained granoblastic domains clearly indicate crystallization in the solid state, but the local presence of relatively coarse igneous-textured leucosome-like patches suggests the former presence of melt locally.

MINERAL CHEMISTRY

Major-element compositions of minerals in selected samples of regional and contact metamorphic rocks (Tables 2–4) were determined by energy-dispersive spectrometry (EDS) using a converted Geoscan electron microprobe operating at 15 kV, 3 nA specimen current on Co metal, and 40 s count time per analysis. X-ray spectra were processed using Link Systems ZAF4/FLS software. In addition, F and Ba contents in biotites in two samples were determined by wavelength-dispersive spectrometry using a Cameca Camebax electron microprobe with fluorite and celsian standards, respectively. Ferric iron contents in garnets and hercynites were calculated by specifying fixed cation-to-oxygen ratios of, respectively, 16:24 and 3:4 (Droop, 1987).

Regional metamorphic rocks

Minerals were analysed in two garnet–biotite gneisses (Sin1, Sin2) and one garnet–mica schist (Sin101) from Cairnie, and three mica schists (Bog1, Clas66 and Clas112) from Clashmach Hill.

Garnet

Garnet crystals in the Cairnie rocks are virtually unzoned. Those in Sin 1 and Sin101 have compositions close to $Alm_{70}Py_{23}Sps_{05}Grs_{01}Adr_{01}$, whereas those of Sin2 cluster around $Alm_{76}Py_{13}Sps_{08}Grs_{03}$. The garnets in Clas66 are also unzoned, but differ from those at Cairnie in their high Mn and low Mg contents; their compositions are close to $Alm_{57}Py_{08}Sps_{31}Grs_{02}Adr_{02}$.

Staurolite

Staurolite in Sin101 has an Mg-number value [$= 100\,Mg/(Fe^{2+} + Mg)$] ranging from 21 to 26 over several grains and contains a small amount of Zn [0·10–0·19 atoms per 48(O)]. The staurolite in Clas66 has Mg-number ranging from 14 to 16 and contains up to 0·19 a.p.f.u. (atoms per formula unit) Zn.

Andalusite

Andalusite in Clas66 contains detectable Fe and Mg impurities (up to 0·01 a.p.f.u. of each).

Biotite

Al^{VI} contents of all analysed regional-metamorphic biotites are closely grouped, mostly between 0·75 and 1·0 atoms per 22(O). Biotites from Cairnie have higher Mg-number values (50–62) and lower Ti contents (0·17–0·25 a.p.f.u.) than those from Clashmach Hill (0·29–0·40 and 0·26–0·40, respectively).

Muscovite

Regional muscovites are all mildly phengitic, with 6·06–6·14 Si and 0·15–0·56 Fe + Mg per 22(O), and contain some Na in their A sites [Na/(Ca + Na + K) = 0·06–0·16 in the Clashmach Hill schists and 0·19–0·26 in Sin2].

Plagioclase

Plagioclases in both Sin1 and Sin2 range from An_{17} to An_{23}. K contents are below the detection limit. Rims and cores of individual grains have similar compositions. Plagioclases in Clas66 are also uniform, with compositions lying in the range $An_{17–21}$.

Contact metamorphic rocks

Analyses of coexisting minerals were obtained from the Sil–Crd hornfels (Dun1), a Crd–Kfs hornfels (Cor8), six Opx–Crd hornfelses (Cor10, BQ17, BQ41, BHQ5, Pir1 and Pir4), and six cordierite norites (BHQ1, BQ38, Dun4, Dun12, CasB2i and CasB5). With a few exceptions, minerals in individual rocks are unzoned and show small within-sample variation, assumed to reflect a close approach to chemical equilibrium.

Garnet

Garnets in Sil–Crd and Crd–Kfs hornfelses display slight zonation, with broad cores of uniform composition (approximately $Alm_{73}Py_{17}Sps_{05}Grs_{04}Adr_{01}$ in Dun1 and $Alm_{79}Py_{16}Sps_{01}Grs_{04}$ in Cor8) and rims up to 1 mm wide, displaying a smooth increase in Fe and decrease in Mg (Fig. 5a), indicating retrograde diffusional exchange.

Garnets in Opx–Crd hornfelses are remarkably unzoned (Fig. 5b) and show little within-sample variation. The Mg-number is typically between 24 and 29, with X_{Ca} between 0·02 and 0·05.

Garnets in cordierite norites are also typically unzoned (Fig. 5c) and similar in composition to those of Opx–Crd hornfelses. The Mg-number is generally

Table 2: Representative electron-microprobe analyses of minerals in regional metamorphic rocks outside the Huntly Complex and in a sillimanite–cordierite hornfels (Dun1)

	Sin2 Grt	Sin2 Bt	Sin2 Ms	Sin2 Pl	Bog1 Bt	Bog1 Ms	Clas112 Bt	Clas112 Ms	Clas66 Grt	Clas66 St	Clas66 Bt	Clas66 Ms	Clas66 Pl	Dun1 Grt	Dun1 Crd	Dun1 Bt	Dun1 Pl
SiO_2	37·41	35·86	45·75	62·62	34·32	45·67	33·95	45·03	36·89	27·02	35·09	45·72	61·58	37·52	49·17	35·85	55·35
TiO_2	0·00	1·65	0·66	n.a.	2·52	1·37	2·70	0·74	0·00	0·78	2·66	0·97	0·00	0·00	0·00	1·74	n.a.
Al_2O_3	20·92	19·25	35·54	23·60	19·14	35·52	19·15	34·96	20·59	53·62	18·52	34·63	23·01	21·12	33·36	19·71	27·97
Cr_2O_3	0·00	0·00	0·07	n.a.	0·00	0·00	0·00	0·09	0·00	0·01	0·00	0·00	0·00	0·03	0·05	0·02	n.a.
Fe_2O_3	0·00	—	—	—	—	—	—	—	0·59	—	—	—	—	0·25	—	—	—
FeO	34·27	18·23	1·49	n.a.	22·08	1·00	21·89	1·39	25·18	13·13	20·87	1·24	0·18	32·99	9·77	17·41	n.a.
MnO	3·65	0·00	0·00	n.a.	0·00	0·00	0·00	0·11	13·57	0·51	0·00	0·00	0·00	2·31	0·00	0·00	n.a.
MgO	3·02	10·73	0·84	n.a.	7·32	0·66	7·49	0·66	1·87	1·42	8·44	0·98	0·00	4·16	7·82	11·11	n.a.
CaO	1·09	0·07	0·07	4·71	0·11	0·00	0·00	0·14	1·45	0·00	0·12	0·11	4·33	1·64	n.a.	0·07	10·04
Na_2O	n.a.	0·68	1·72	8·96	0·45	1·20	0·57	0·91	n.a.	0·10	0·38	0·49	9·23	n.a.	n.a.	0·63	5·79
K_2O	n.a.	8·92	8·76	0·02	8·83	9·71	8·88	9·85	n.a.	0·01	9·09	10·44	0·10	n.a.	n.a.	8·99	0·00
Total	100·36	95·38	94·90	99·91	94·77	95·13	94·63	93·88	100·13	97·51	95·16	94·58	98·43	100·02	100·17	95·53	99·22
Formula	24(O)	22(O)	22(O)	8(O)	22(O)	22(O)	22(O)	22(O)	24(O)	48(O)	22(O)	22(O)	8(O)	24(O)	18(O)	22(O)	8(O)
Si	6·01	5·41	6·09	2·77	5·32	6·08	5·28	6·09	6·00	7·89	5·39	6·14	2·77	6·00	5·00	5·38	2·51
Ti	0·00	0·19	0·07	n.a.	0·29	0·14	0·32	0·08	0·00	0·17	0·31	0·10	0·00	0·00	0·00	0·20	n.a.
Al	3·97	3·42	5·58	1·23	3·50	5·57	3·51	5·57	3·94	18·46	3·35	5·48	1·22	3·98	3·99	3·48	1·49
Cr	0·00	0·00	0·01	n.a.	0·00	0·00	0·00	0·01	0·00	0·00	0·00	0·00	0·00	0·00	0·00	0·00	n.a.
Fe^{3+}	0·00	—	—	—	—	—	—	—	0·07	—	—	—	—	0·03	—	—	—
Fe^{2+}	4·61	2·30	0·17	n.a.	2·86	0·11	2·85	0·16	3·42	3·21	2·68	0·14	0·01	4·41	0·83	2·18	n.a.
Mn	0·50	0·00	0·00	n.a.	0·00	0·00	0·00	0·01	1·87	0·13	0·00	0·00	0·00	0·31	0·00	0·00	n.a.
Mg	0·72	2·41	0·17	n.a.	1·69	0·13	1·74	0·13	0·45	0·62	1·93	0·20	0·00	0·99	1·18	2·48	n.a.
Ca	0·19	0·01	0·01	0·22	0·02	0·00	0·00	0·02	0·25	0·00	0·02	0·02	0·21	0·28	n.a.	0·01	0·49
Na	n.a.	0·20	0·44	0·77	0·14	0·31	0·17	0·24	n.a.	0·06	0·11	0·13	0·81	n.a.	n.a.	0·18	0·51
K	n.a.	1·72	1·49	0·00	1·75	1·65	1·76	1·70	n.a.	0·00	1·78	1·79	0·01	n.a.	n.a.	1·72	0·00
Total	16·00	15·66	14·03	4·99	15·57	13·99	15·63	14·01	16·00	30·74	15·57	14·00	5·03	16·00	11·00	15·63	5·00

n.a., not analysed.

Table 3: Representative electron-microprobe analyses of minerals in orthopyroxene–cordierite hornfelses in the Huntly Complex

	BHQ5 Grt	BHQ5 Opx	BHQ5 Crd	BHQ5 Hc	BHQ5 Bt	BHQ5 Pl	BQ17 Grt	BQ17 Opx	BQ17 Crd	BQ17 Hc	BQ17 Pl	BQ17 Kfs	BQ41 Grt	BQ41 Opx	BQ41 Crd	BQ41 Fsp
SiO_2	38·38	47·21	48·89	0·03	36·10	57·42	37·91	47·10	48·53	0·15	57·95	64·62	37·90	46·82	48·86	64·74
TiO_2	0·03	0·30	0·00	0·09	6·63	n.a.	0·03	0·27	0·07	0·00	n.a.	n.a.	0·18	0·41	0·00	n.a.
Al_2O_3	21·42	6·17	33·07	57·89	15·77	27·25	21·36	5·97	32·90	56·74	26·46	19·56	21·30	6·53	32·96	21·11
Cr_2O_3	0·09	0·10	0·00	0·96	0·09	n.a.	0·06	0·09	0·00	0·40	n.a.	n.a.	0·09	0·17	0·00	n.a.
Fe_2O_3	0·23	—	—	3·92	—	—	0·18	—	—	4·47	—	—	0·00	—	—	—
FeO	32·18	31·63	8·71	28·06	15·99	n.a.	31·88	32·17	8·68	29·87	n.a.	n.a.	33·52	32·73	8·68	n.a.
MnO	0·84	0·00	0·10	0·00	0·09	n.a.	0·66	0·00	0·00	0·00	n.a.	n.a.	0·23	0·00	0·00	n.a.
MgO	6·22	14·16	8·50	7·35	10·87	n.a.	6·47	13·74	8·56	6·00	n.a.	n.a.	6·01	13·03	8·26	n.a.
CaO	1·40	0·23	n.a.	n.a.	0·01	9·09	0·99	0·06	n.a.	n.a.	8·44	0·42	0·72	0·05	n.a.	2·12
Na_2O	n.a.	n.a.	n.a.	n.a.	0·22	6·37	n.a.	n.a.	n.a.	n.a.	6·58	0·99	n.a.	n.a.	n.a.	7·65
K_2O	n.a.	n.a.	n.a.	n.a.	9·18	0·32	n.a.	n.a.	n.a.	n.a.	0·40	14·83	n.a.	n.a.	n.a.	4·11
ZnO	n.a.	n.a.	n.a.	2·39	n.a.	n.a.	n.a.	n.a.	n.a.	2·36	n.a.	n.a.	n.a.	n.a.	n.a.	n.a.
Total	100·77	99·80	99·27	100·68	94·95	100·45	99·52	99·40	98·76	99·99	99·82	100·42	99·94	99·74	98·76	99·73
Formula	24(O)	6(O)	18(O)	4(O)	22(O)	8(O)	24(O)	6(O)	18(O)	4(O)	8(O)	8(O)	24(O)	6(O)	18(O)	8(O)
Si	6·01	1·84	4·99	0·00	5·44	2·56	5·99	1·86	4·98	0·00	2·60	2·96	5·99	1·84	5·01	2·89
Ti	0·00	0·01	0·00	0·00	0·75	n.a.	0·00	0·01	0·01	0·00	n.a.	n.a.	0·02	0·01	0·00	n.a.
Al	3·95	0·28	3·99	1·89	2·80	1·43	3·98	0·28	3·98	1·89	1·40	1·06	3·97	0·30	3·98	1·11
Cr	0·01	0·00	0·00	0·02	0·01	n.a.	0·01	0·00	0·00	0·01	n.a.	n.a.	0·01	0·01	0·00	n.a.
Fe^{3+}	0·03	—	—	0·08	—	—	0·02	—	—	0·10	—	—	0·00	—	—	—
Fe^{2+}	4·21	1·03	0·74	0·65	2·02	n.a.	4·21	1·06	0·74	0·70	n.a.	n.a.	4·43	1·08	0·74	n.a.
Mn	0·11	0·00	0·01	0·00	0·01	n.a.	0·09	0·00	0·00	0·00	n.a.	n.a.	0·03	0·00	0·00	n.a.
Mg	1·45	0·82	1·29	0·31	2·44	n.a.	1·53	0·81	1·31	0·25	n.a.	n.a.	1·42	0·76	1·26	n.a.
Ca	0·23	0·01	n.a.	n.a.	0·00	0·44	0·17	0·00	n.a.	n.a.	0·41	0·02	0·12	0·00	n.a.	0·10
Na	n.a.	n.a.	n.a.	n.a.	0·07	0·55	n.a.	n.a.	n.a.	n.a.	0·57	0·09	n.a.	n.a.	n.a.	0·66
K	n.a.	n.a.	n.a.	n.a.	1·77	0·02	n.a.	n.a.	n.a.	n.a.	0·02	0·87	n.a.	n.a.	n.a.	0·23
Zn	n.a.	n.a.	n.a.	0·05	n.a.	n.a.	n.a.	n.a.	n.a.	0·05	n.a.	n.a.	n.a.	n.a.	n.a.	n.a.
Total	16·00	4·01	11·02	3·00	15·31	5·00	16·00	4·02	11·02	3·00	5·00	5·00	15·99	4·00	10·99	4·99

n.a., not analysed.

Table 4: Representative electron-microprobe analyses of minerals in cordierite norites of the Huntly Complex

	BQ38 Grt	BQ38 Opx	BQ38 Crd	BQ38 Hc	BQ38 Bt	BQ38 Pl	CasB5 Grt	CasB5 Opx	CasB5 Crd	CasB5 Hc	CasB5 Bt	CasB5 Pl	Dun4 Grt	Dun4 Opx	Dun4 Crd	Dun4 Bt	Dun4 Pl
SiO_2	38·60	48·11	48·71	0·00	36·11	53·35	38·46	49·63	49·35	0·00	36·11	54·44	38·14	48·69	49·35	36·21	54·03
TiO_2	0·00	0·25	0·00	0·00	4·12	n.a.	0·00	0·14	0·00	0·00	4·98	n.a.	0·15	0·21	0·00	3·68	n.a.
Al_2O_3	21·79	5·86	32·96	56·81	17·44	29·63	21·79	4·22	33·22	59·24	16·12	29·52	21·35	4·03	33·34	16·69	29·73
Cr_2O_3	0·00	0·18	0·00	0·75	0·25	n.a.	0·00	0·00	0·00	0·00	0·00	n.a.	0·01	0·13	0·00	0·05	n.a.
Fe_2O_3	0·13	—	—	4·08	—	—	0·85	—	—	2·80	—	—	0·58	—	—	—	—
FeO	31·72	30·88	8·14	31·03	18·14	n.a.	28·25	27·28	6·85	29·60	15·74	0·12	32·19	30·27	7·37	14·34	n.a.
MnO	0·79	0·00	0·00	0·00	0·03	n.a.	1·89	0·44	0·00	0·00	0·00	n.a.	0·30	0·00	0·00	0·00	n.a.
MgO	6·66	15·23	8·80	5·54	10·91	n.a.	7·66	17·74	9·70	6·55	13·04	n.a.	5·98	15·73	9·30	14·06	n.a.
CaO	1·36	0·17	n.a.	0·00	0·06	12·23	1·70	0·26	n.a.	0·00	0·00	11·70	2·00	0·19	n.a.	0·13	11·56
Na_2O	n.a.	n.a.	n.a.	n.a.	0·00	4·63	n.a.	n.a.	n.a.	n.a.	0·55	5·15	n.a.	n.a.	n.a.	0·50	5·03
K_2O	n.a.	n.a.	n.a.	n.a.	9·46	0·15	n.a.	n.a.	n.a.	n.a.	8·91	0·07	n.a.	n.a.	n.a.	8·65	0·00
ZnO	n.a.	n.a.	n.a.	1·42	n.a.	n.a.	n.a.	n.a.	n.a.	2·10	n.a.	n.a.	n.a.	n.a.	n.a.	n.a.	n.a.
Total	101·04	100·67	98·60	99·64	97·03*	99·98	100·58	99·70	99·12	100·28	95·44	101·01	100·70	99·24	99·36	94·31	100·34
Formula	24(O)	6(O)	18(O)	4(O)	22(O)	8(O)	24(O)	6(O)	18(O)	4(O)	22(O)	8(O)	24(O)	6(O)	18(O)	22(O)	8(O)
Si	6·00	1·85	4·99	0·00	5·40	2·41	5·96	1·90	5·00	0·00	5·40	2·44	5·97	1·90	5·00	5·43	2·43
Ti	0·00	0·01	0·00	0·00	0·46	n.a.	0·00	0·00	0·00	0·00	0·56	n.a.	0·02	0·01	0·00	0·42	n.a.
Al	3·99	0·27	3·98	1·90	3·07	1·58	3·98	0·19	3·97	1·94	2·84	1·56	3·94	0·18	3·98	2·77	1·58
Cr	0·00	0·01	0·00	0·02	0·03	n.a.	0·00	0·00	0·00	0·00	0·00	n.a.	0·00	0·00	0·00	0·00	n.a.
Fe^{3+}	0·02	—	—	0·09	—	—	0·10	—	—	0·06	—	—	0·07	—	—	—	—
Fe^{2+}	4·12	0·99	0·70	0·73	2·27	n.a.	3·66	0·87	0·58	0·69	1·97	0·00	4·22	0·99	0·62	3·67	n.a.
Mn	0·10	0·00	0·00	0·00	0·00	n.a.	0·25	0·01	0·00	0·00	0·00	n.a.	0·04	0·00	0·00	0·00	n.a.
Mg	1·54	0·87	1·34	0·23	2·43	n.a.	1·77	1·01	1·47	0·27	2·91	n.a.	1·40	0·91	1·41	1·27	n.a.
Ca	0·23	0·01	n.a.	0·00	0·01	0·59	0·28	0·01	n.a.	0·00	0·00	0·56	0·34	0·01	n.a.	0·04	0·56
Na	n.a.	n.a.	n.a.	n.a.	0·00	0·41	n.a.	n.a.	n.a.	n.a.	0·16	0·45	n.a.	n.a.	n.a.	0·13	0·44
K	n.a.	n.a.	n.a.	n.a.	1·80	0·01	n.a.	n.a.	n.a.	n.a.	1·70	0·00	n.a.	n.a.	n.a.	1·74	0·00
Zn	n.a.	n.a.	n.a.	0·03	n.a.	n.a.	n.a.	n.a.	n.a.	0·04	n.a.	n.a.	n.a.	n.a.	n.a.	n.a.	n.a.
Total	16·00	4·01	11·01	3·00	15·47	5·00	16·00	3·99	11·02	3·00	15·54	5·01	16·00	4·00	11·01	15·57	5·01

*Includes 0·02 wt % Cl, 0·24 wt % F and 0·27 wt % BaO.
n.a., not analysed.

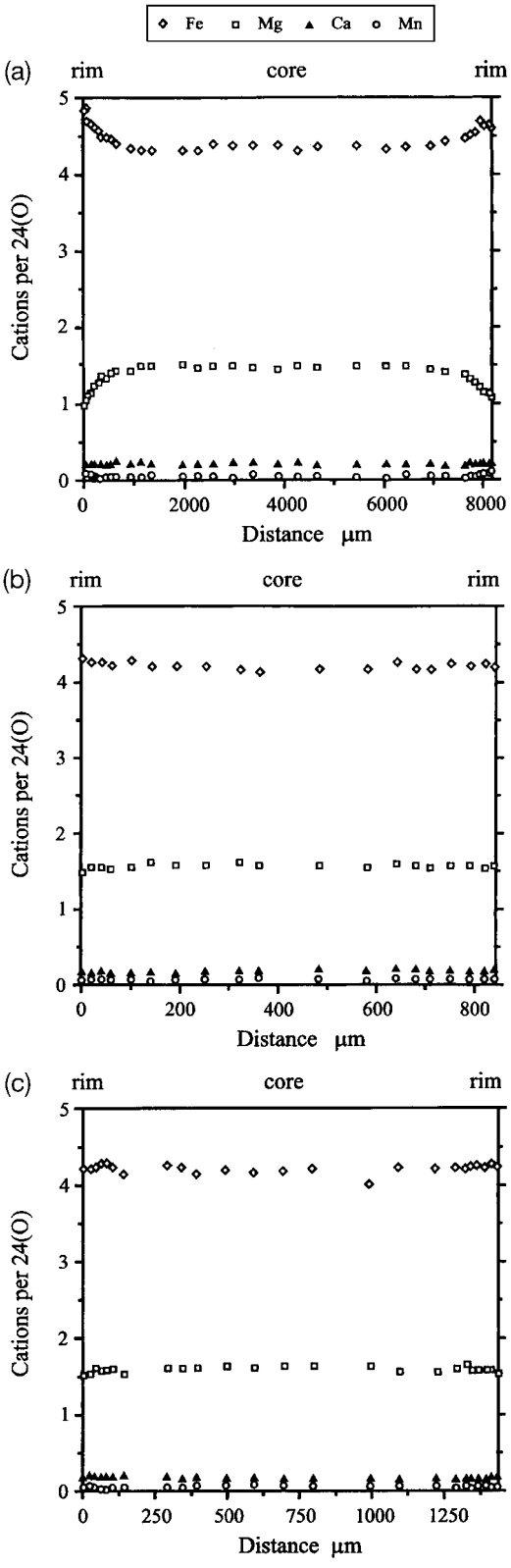

Fig. 5. Zoning profiles across garnets in pelitic rocks of the Huntly Complex. (a) Sil–Crd hornfels Cor8; (b) Opx–Crd hornfels BQ17; (c) Crd norite BHQ1.

between 26 and 30, Mn contents are low (X_{Mn} mostly between 0·004 and 0·02) and X_{Ca} ranges from 0·027 to 0·068.

Orthopyroxene

The Mg-number and X_{Al}^{M1} contents of orthopyroxenes from all the Opx–Crd hornfelses are similar, ranging from 40 to 50 and from 0·07 to 0·18, respectively. Cation totals cluster around 4·00 per 6(O), suggesting that Fe^{3+} contents are very low.

Orthopyroxenes from cordierite norites are generally very similar to those of Opx–Crd hornfelses; Mg-number generally varies from 45 to 52, except in CasB2i, in which it varies from 50 to 58, and X_{Al}^{M1} is typically between 0·05 and 0·18. X_{Ca}^{M2} is low, rarely exceeding 0·01.

Cordierite

The Mg-number values of the two analysed Opx-free hornfelses are similar, ranging from 60 to 68 in Cor8 and from 59 to 71 in Dun1. The cordierites in the Opx–Crd hornfelses are slightly more magnesian, Mg-number varying from 63 to 72 in BQ17, from 61 to 64 in BQ41, and from 61 to 66 in BHQ5 and Pir1. The Mg-number values of cordierites in the cordierite norites overlap substantially with these ranges (62–67 in BHQ1, 72–73 in CasB2i, 63–67 in BQ38 and 71–73 in CasB5). No significant zoning has been detected.

Thermogravimetric determination of total volatile content was carried out for cordierites in two samples: cordierite norite BQ38, and cordieritite 10035. Fifteen milligram aliquots of powdered sample were heated under Ar (to prevent oxidation) and held at 900°C for at least 30 min. The measured mass losses were 1·07% for BQ38 and 0·65% for 10035. H_2O and CO_2 are known to be able to occupy the channel site in cordierite (e.g. Schreyer & Yoder, 1964; Johannes & Schreyer, 1981; Vry *et al.*, 1990) and are thus the volatile species most likely to have been present. The 1·07% weight loss for BQ38 is equivalent to a maximum X_{H_2O} value of 0·36 or a maximum X_{CO_2} value of 0·15. For 10035, the data imply a maximum X_{H_2O} value of 0·22 or a maximum X_{CO_2} value of 0·092.

Biotite

Biotites in the Sil–Crd and Crd–Kfs hornfelses have Al^{VI} contents of between 0·67 and 1·46 a.p.f.u. [22(O)]. The Mg-number values range from 44 to 51 in Cor8 and from 54 to 55 in Dun1. Ti contents are relatively low (0·16–0·54 a.p.f.u.). Biotites in contact with garnet generally have higher Mg-number than those remote from garnet, complementing the Fe-rich

garnet rims, and confirming that there has been retrograde Fe–Mg exchange.

Biotites in Opx–Crd hornfelses are less aluminous than those of Opx-free hornfelses, with Al^{VI} contents of between 0·24 and 0·35. The Mg-number ranges from 48 to 57, and Ti contents are high (0·57–0·75 a.p.f.u.). Biotites in cordierite norites have similar Mg-number but slightly higher Al^{VI} contents. Again, biotites closest to garnet are richest in Mg. Ba and F were determined in the biotites of two cordierite norites; X_F in biotites in BHQ1 range from 0·017 to 0·061, and those in BQ38 from 0·014 to 0·052. Ba contents in both samples are $<0·5$ wt %.

Hercynite and sillimanite

All analysed spinels are rich in the $FeAl_2O_4$ component, with low Cr [0·01–0·05 per 4(O)] and Zn (0·03–0·07 a.p.f.u.), and barely detectable Ti. Calculated Fe^{3+} contents are $<0·12$ a.p.f.u. The Mg-number values of hercynites in Opx–Crd hornfelses range from 26 to 27 (BQ17), from 16 to 25 (Pir1) and from 18 to 32 (BHQ5); those of hercynites in cordierite norites are similar, ranging from 22 to 29. Sillimanites in Dun1 and Cor8 are virtually pure, with no significant Fe^{3+} or Mn^{3+} substitution.

Feldspars

Three compositional types of feldspar occur in the thermally metamorphosed rocks: plagioclase, K-feldspar and anorthoclase. The plagioclases in the Sil–Crd and Crd–Kfs hornfelses are andesines; those of Cor8 show mild normal zonation from An_{46} cores to An_{34} rims. The compositions of small plagioclase grains in Opx–Crd hornfelses Pir1 and Pir4 are tightly clustered between An_{34} and An_{38}; those of large plagioclases in BQ17 are more variable ($An_{35–40}Or_{02–08}$) (Fig. 6a). The plagioclases in the cordierite norites are commonly strongly zoned, with distinct An-rich cores and Ab-rich rims. In BQ38, for example, compositions range from An_{59} to An_{41} (Fig. 6b) and in Dun12 they range from An_{74} to An_{49}. Oscillatory zoning occurs within both core and rim regions. Such zoning patterns are normally present only in plagioclases from igneous rocks, rimward enrichment in Na being commonly interpreted as reflecting decreasing temperatures during crystallization. These zoning patterns therefore strongly suggest that the plagioclases in Crd norites crystallized in the presence of melt, with rims crystallizing during cooling.

K-feldspars in hornfelses Cor8 and BQ17 have compositions $Or_{81–85}$ and $Or_{87–90}$, respectively, whereas those in cordierite norite BHQ1 are $Or_{82–88}$. The composition of the anorthoclase in BQ41 is variable within the thin section, ranging in a linear fashion mainly between $Or_{50}Ab_{43}An_{07}$ and $Or_{24}Ab_{66}An_{10}$. No twinning or optical zoning is apparent in either type of feldspar.

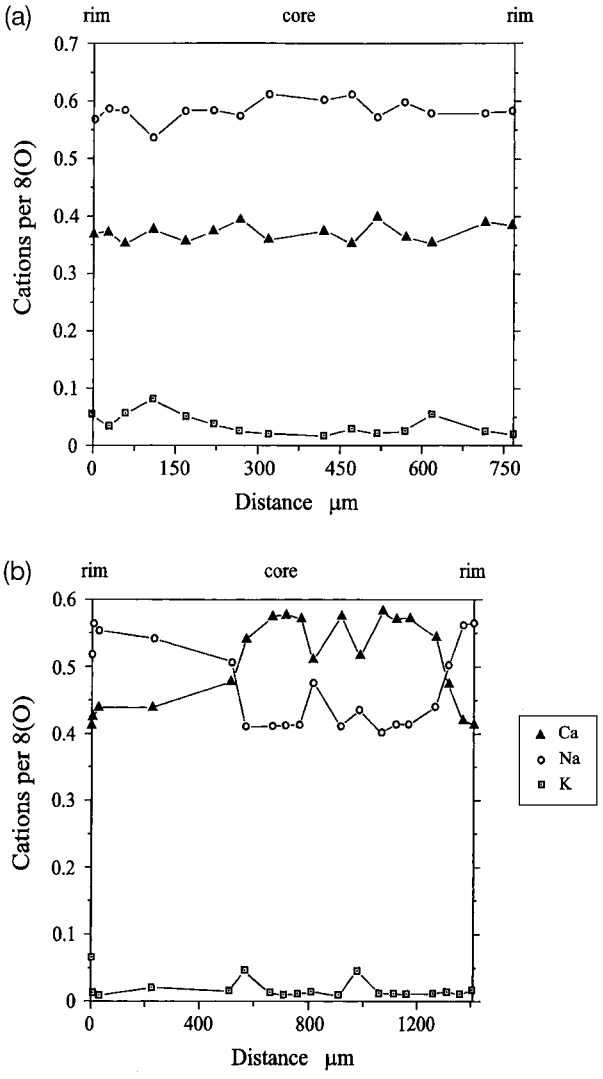

Fig. 6. Zoning profiles across plagioclase crystals in metapelitic rocks of the Huntly Complex. (a) Opx–Crd hornfels BQ17; (b) Grt–Crd norite BQ38.

Ilmenite

All analysed ilmenites are close to the $FeTiO_3$ endmember in composition. Fe^{2+} contents invariably exceed 0·96 atoms per 3(O), the main diluent being Mg.

P–T–a$_{H_2O}$ CONDITIONS OF METAMORPHISM

In this section, mineral equilibria are used to estimate the peak *P–T* conditions of Grampian regional

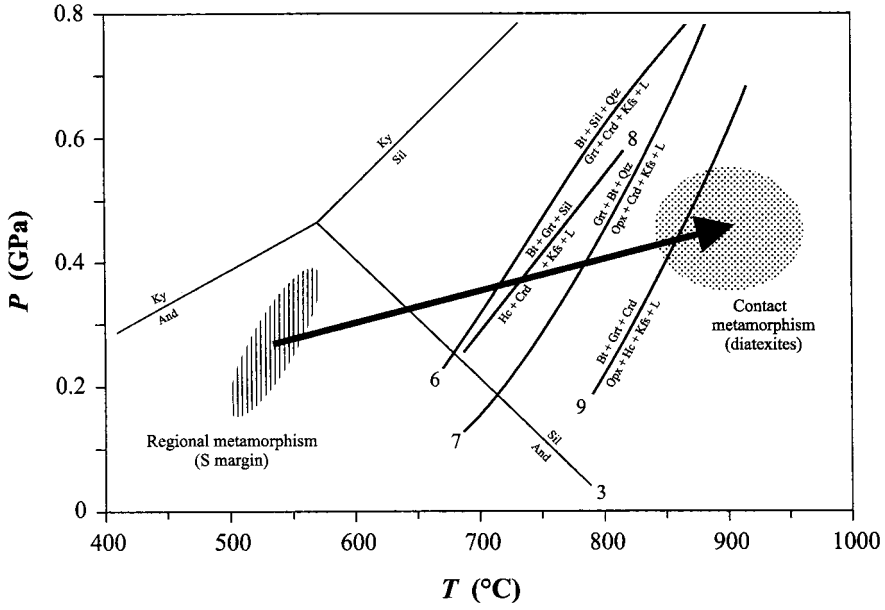

Fig. 7. Metamorphic P–T conditions recorded by pelitic rocks in the southern segment of the Huntly Complex. Dotted area: peak contact-metamorphic conditions estimated for Opx-bearing rocks; lined area: peak regional-metamorphic conditions, based on schist sample Clas66. Arrow: deduced prograde P–T path. Numbers identify reactions discussed in the text. Qtz-present melting reaction curves from Holland *et al.* (1996); Hc-present melting curves are from this study. Calculations by White *et al.* (2001) suggest that reactions (6) and (7) [and, by implication, (8) and (9)] are slightly steeper than shown and occur at temperatures ~15°C higher at 0·4 GPa than shown.

metamorphism in the country rocks of the Huntly Complex, and the peak P–T–a_{H_2O} conditions of contact metamorphism in hornfelses and migmatites. The results provide information on (1) the thermal state of the country rocks before intrusion, (2) the crustal level of emplacement of the gabbros, (3) the conditions of migmatization, and (4) the P–T path followed by the rocks.

P–T conditions of Grampian regional metamorphism

Peak-metamorphic conditions of regional rocks to the west and south of the Huntly Complex were estimated by applying version 2.75 (1998) of the program THERMOCALC (Powell & Holland, 1988; Holland & Powell, 1998), in 'average P–T mode', to coexisting minerals in schists Clas66 and Sin2. Activity models used were Berman (1990) for grossular, almandine and pyrope components in garnet, Elkins & Grove (1991) for anorthite in plagioclase, Holland & Powell (1990) for muscovite and ferroceladonite in muscovite [with non-ideal parameters for alkali-sites from Chatterjee & Flux (1986)], Holland & Powell (1990) for annite, phlogopite and eastonite in biotite, and ideal ionic mixing for staurolite. Andalusite, quartz and H_2O activities were assumed to be unity.

On the basis of five independent equilibria, the best-fit results for andalusite schist Clas66, from the south of the complex, are $T = 537 \pm 42$°C and $P = 0{\cdot}27 \pm 0{\cdot}12$ GPa (Fig. 7), with a fit index (f) of 0·88, which, passing the χ^2 test, indicates that the averaging is reasonable with 95% confidence. These results are consistent with those of Hudson (1985) for andalusite-zone rocks on the Banff coast. The pressure value implies a depth of burial of $\sim 10 \pm 4$ km before gabbro intrusion. Five independent equilibria in sillimanite-zone schist Sin2, from the west of the complex, gave a best fit of 637 ± 31°C and $0{\cdot}65 \pm 0{\cdot}13$ GPa ($f = 0{\cdot}25$). The pressure difference between localities on the south and west of the complex is consistent with the abrupt change in regional metamorphic character across the Portsoy–Duchray Lineament noted by Harte & Hudson (1979) and Beddoe-Stephens (1990).

P–T conditions of contact metamorphism

Peak contact-metamorphic conditions in the non-migmatitic hornfels and the highest-grade (Opx-bearing) migmatites were estimated using THERMOCALC and independently calibrated thermobarometers. The latter include the Grt–Bt (Bhattacharya *et al.*, 1992), Grt–Crd (Nichols *et al.*, 1992), Grt–Opx (Bhattacharya *et al.*, 1991) Fe,Mg-exchange geothermometers, the Opx(Al)–Grt geothermometer (Harley &

Table 5: Thermobarometric data for contact metamorphism

	T (°C) Grt–Bt (FM) Bh.'92	*T* (°C) Grt–Crd (FM) Ni.'92	*T* (°C) Grt–Opx (FM) Bh.'91	*T* (°C) Grt–Opx (Al) H&G'82	*P* (GPa) GOPQ (Fe) Bh.'91	*P* (GPa) GOPQ (Mg) Bh.'91	Best-fit *T* (°C) & *P* (GPa) GCOHP Th.'98
Crd norites							
BHQ1	753	819	848	859	0·52	0·55	922 (±81) 0·47 (±0·10)
BQ38	758	816	873	878	0·39	0·44	896 (±79) 0·45 (±0·09)
CasB2i	719	788	849	805	0·39	0·52	—
CasB5	718	693	815	797	0·52	0·57	766 (±89) 0·35 (±0·10)
Dun4	655	682	814	828	0·52	0·53	804 (±71) 0·43 (±0·09)
Dun12	705	724	877	880	0·38	0·51	882 (±77) 0·48 (±0·09)
Dun9b	751	—	—	—	—	—	—
Hornfelses							
Cor8	676	715	—	—	—	—	—
Dun1	592	601	—	—	—	—	—
Cor10	738	—	795	787	0·59	0·60	—
BQ17	—	760	883	900	—	—	921 (±84) 0·51 (±0·10)
BQ41	—	789	915	911	—	—	—
BHQ5	—	859	880	882	—	—	913 (±77) 0·44 (±0·09)
Pir1	—	879	960	918	—	—	952 (±90) 0·51 (±0·11)
Pir4	—	—	957	919	—	—	—

Independent calibrations: H&G'82, Harley & Green (1982); Bh.'91, Bhattacharya *et al*. (1991); Bh.'92, Bhattacharya *et al*. (1992); Ni.'92, Nichols *et al*. (1992). FM, Fe,Mg-exchange thermometer; GOPQ, Grt–Opx–Pl–Qtz geobarometer. All temperatures calculated at a reference pressure of 0·45 GPa. Pressures calculated at temperatures given by Grt–Opx (Fe,Mg)-thermometry. Th'98, THERMOCALC v.2.75 in 'average *P*–*T* mode' (Holland & Powell, 1998). GCOHP, best-fit intersection of six independent equilibria involving the restitic assemblage Grt–Crd–Opx–Hc–Pl.

Green, 1982) and the Grt–Opx–Pl–Qtz geobarometer (Bhattacharya *et al*., 1991). For the Grt–Opx–Pl–Qtz geobarometer, end-member activities were calculated using the quaternary mixing model of Berman (1990) for garnet, Elkins & Grove (1991) for plagioclase, and Wood & Banno (1972) for orthopyroxene. Results from most of these calibrations are summarized in Table 5.

Non-migmatitic hornfels

Application of Fe,Mg-exchange geothermometers to Sil–Crd hornfels sample Dun1 yields temperatures in the vicinity of 600°C. In 'average *P*–*T* mode', THERMOCALC yields best-fit conditions of $T = 628 \pm 75$°C and $P = 0{\cdot}51 \pm 0{\cdot}08$ GPa ($f = 0{\cdot}93$) for this rock at an arbitrary a_{H_2O} value of 1·0.

High-grade hornfelses and diatexite matrix rocks

Application of Grt–Opx thermometers to Opx-bearing contact rocks yields temperatures mostly in the range 850–950°C (Table 5). Fe,Mg-exchange thermometers involving biotite and cordierite, on the same samples, generally give significantly lower temperatures, reflecting the susceptibility of such exchange equilibria to retrograde re-equilibration (e.g. Frost & Chacko, 1989; Fitzsimons & Harley, 1994). The anorthoclases of sample BQ41 plot mostly between the 900°C and 970°C isotherms on the 5 kbar ternary feldspar solvus of Elkins & Grove (1991), in agreement with the Grt–Opx thermometry.

Application of the Grt–Opx–Pl–Qtz geobarometer to cores of coexisting minerals in Opx–Crd norites yields pressures [at temperatures given by Grt–Opx (Fe,Mg) thermometry] ranging from 0·39 to 0·57 GPa ($\pm > 0{\cdot}1$ GPa) and averaging $\sim$0·49 GPa, consistent with the results of Ashworth & Chinner (1978) and Droop & Charnley (1985). However, these pressures must be treated with caution because the quartz in these rocks is interstitial and probably crystallized after the garnet, orthopyroxene and plagioclase. As an independent check, *P*–*T* conditions were also calculated using equilibria among end-member components in the quartz-absent restitic assemblage

Grt + Opx + Crd + Hc + Pl in Crd norites and Opx–Crd hornfelses. The following ideal mixing models were used: for cordierite $a_{FeCrd} = (X_{Fe})^2 \cdot X_v$ and $a_{MgCrd} = (X_{Mg})^2 \cdot X_v$, where X_v is the mole fraction of channel-site vacancies, and for hercynite $a_{Hc} = X_{Fe} \cdot (X_{Al})^2$ and $a_{Spl} = X_{Mg} \cdot (X_{Al})^2$. The X_v values for Crd norites and Opx–Crd hornfelses were calculated from the maximum H_2O contents permitted by the gravimetric data in cordierites from BQ38 (0·36 H_2O a.p.f.u.) and 10035 (0·22 H_2O a.p.f.u.), respectively. Best-fit results, calculated using THERMOCALC in 'average *P–T* mode', are mostly in the range 900–950°C, 0·4–0·5 GPa ($f < 1·2$) (Table 5), in agreement with results of Grt–Opx–Pl–Qtz barometry.

The present thermobarometric results for Opx-bearing rocks confirm earlier pressure estimates ($\sim$0·45 ± 0·1 GPa) but indicate that peak temperatures were in the region of 900 ± 50°C, higher than previously thought.

H_2O activity conditions of contact metamorphism

Having estimated peak *P–T* conditions in the Opx-bearing rocks, dehydration equilibria can now be used to estimate a_{H_2O} conditions (Lamb & Valley, 1988). Crd norite BHQ1 contains biotite, quartz, orthopyroxene and K-feldspar, for which the equilibrium

$$\underset{\text{biotite}}{2KMg_3AlSi_3O_{10}(OH)_2} + \underset{\text{quartz}}{6SiO_2} = \underset{\text{Opx}}{3Mg_2Si_2O_6} + \underset{\text{K-feldspar}}{2KAlSi_3O_8} + \underset{\text{melt}}{2H_2O} \quad (1)$$

and its Fe analogue may be written. When a_{H_2O} isopleths for (1) are calculated for mineral compositions in BHQ1, the field of peak *P–T* conditions intersects the $a_{H_2O} = 0·1$ isopleth. The Fe analogue of (1) yields a somewhat higher a_{H_2O} value of $\sim$0·3. At 830°C, arguably a more realistic temperature for the crystallization of interstitial quartz and K-feldspar and poikilitic biotite around orthopyroxene, lower a_{H_2O} values are implied ($\sim$0·06 and 0·2 for Mg- and Fe-end-member versions, respectively). The data of Clemens & Wall (1981) yield a_{H_2O} values of 0·33–0·42 for K-feldspar crystallization at the expense of Opx and melt over a temperature range of 845–820°C at 0·5 GPa in an S-type granitic system.

The low volatile contents of cordierites also provide evidence for low values of a_{H_2O} in the highest-grade rocks. Application of the H_2O–cordierite data of Harley *et al.* (2002) to BQ38 and 10035 cordierites at 900°C and 0·45 GPa yields maximum a_{H_2O} values of 0·27 and 0·13, respectively. The H_2O contents of granitic melts under those conditions, calculated using the 900°C, 0·5 GPa cordierite–melt partitioning data of Carrington & Harley (1996), are 4·5 and 2·9 wt %, respectively, significantly lower than those of H_2O-saturated eutectic haplogranitic melt (Holtz & Johannes, 1994).

REACTION HISTORY

In this section we use textural evidence and established chemographic relations to reconstruct the mineralogical changes that took place as the Dalradian metapelites, in the vicinity of the Huntly Complex, were thermally metamorphosed and partially melted by the gabbro intrusion.

Subsolidus reactions

The sillimanite pseudomorphs after andalusite in Dun1 provide textural evidence for the conversion of regional andalusite-bearing schists, such as outcrop south of the Huntly Complex, into Sil–Crd hornfels. The simplest set of KFMASH discontinuous reactions by which the dominant regional And + St + Bt + Ms + Pl + Qtz assemblage could have been converted into Grt + Crd + Sil + Bt + Pl + Qtz is as follows:

$$\text{And} = \text{Sil} \quad (2)$$

$$\text{St} + \text{Ms} + \text{Qtz} = \text{Grt} + \text{And/Sil} + \text{Bt} + H_2O \quad (3)$$

and

$$\text{St} + \text{Qtz} = \text{Grt} + \text{Crd} + \text{And/Sil} + H_2O. \quad (4)$$

Reactions (3) and (4) must have occurred in the stated sequence, but the relative timing of reaction (2) is unconstrained.

Partial melting reactions

The assemblage biotite + Al-silicate + quartz, which characterizes many regional schists and the non-migmatitic hornfels, does not appear to occur in equilibrium in the migmatites. The widespread occurrence of garnetiferous leucosomes in the metatexites (Fig. 3b) and of large sub/euhedral garnets and cordierites in the garnet tonalites (Fig. 3c) suggests that this assemblage

was destroyed by the incongruent, fluid-absent melting reactions

$$\text{Bt} + \text{Sil} + \text{Qtz} = \text{Grt} + \text{Kfs} + \text{melt} \quad (5)$$

and

$$\text{Bt} + \text{Sil} + \text{Qtz} = \text{Grt} + \text{Crd} + \text{Kfs} + \text{melt}. \quad (6)$$

KFMASH discontinuous reaction (6) has been implicated in many garnetiferous migmatites (e.g. Waters & Whales, 1984; Waters, 1988; Powell & Downes, 1990) and is known to occur in metapelites of 'normal' compositions when they are heated at moderate pressures (Thompson, 1982; Grant, 1985*a*, 1985*b*; Vielzeuf & Holloway, 1988; Patiño Douce & Johnston, 1991; Holland *et al*., 1996; Johnson *et al*., 2001*a*). The existence of plagioclase in the hornfels melanosomes means that reactions (5) and (6) are likely to have involved this phase, in addition to those listed (Patiño Douce & Beard, 1996; White *et al*., 2001), with relatively Na-rich plagioclase as a reactant, and relatively Ca-rich plagioclase and Na,Ca-bearing melt as product phases. When Na_2O and CaO are added to the KFMASH system, discontinuous reactions such as (6) [and reactions (7)–(9), below] become continuous, if plagioclase is the only additional phase.

There is no textural or mineralogical evidence for any further melting reactions in the metatexites and garnet tonalites. However, the crystallization of orthopyroxene and hercynite in the cordierite norites and Opx–Crd hornfelses requires that further melting reactions occurred, and indicates that these rocks experienced even higher grades of metamorphism.

In relatively siliceous, low-alumina rocks, sillimanite is likely to be the first mineral to be consumed in reaction (6). Further heating would then result in incongruent, fluid-absent melting of biotite + garnet + quartz (Grant, 1985*a*, 1985*b*; Holland *et al*., 1996):

$$\text{Bt} + \text{Grt} + \text{Qtz} = \text{Opx} + \text{Crd} + \text{Kfs} + \text{melt}. \quad (7)$$

The occurrence of this reaction would account for the following features of the hercynite-free cordierite norites: (1) the abundance of large, subhedral, 'cumulus' orthopyroxenes and cordierites; (2) the corresponding scarcity of garnets; (3) the rarity of non-interstitial biotite and quartz.

In relatively aluminous, silica-poor rocks, quartz may be exhausted before biotite or sillimanite in reaction (6). In these rocks, instead of reaction (7), further heating would result in incongruent melting of biotite + sillimanite + garnet to produce a quartz-free solid product assemblage (Pattison & Tracy, 1991; Srogi *et al*., 1993):

$$\text{Bt} + \text{Sil} + \text{Grt} = \text{Crd} + \text{Hc} + \text{Kfs} + \text{melt}. \quad (8)$$

Textural evidence for the occurrence of this reaction is provided by the replacement of sillimanite by Hc + Crd aggregates (Fig. 4a), particularly in Opx-free diatexite matrix rocks (e.g. Fow1, Table 1).

On further heating, any biotite remaining after reactions (7) and (8) would ultimately be consumed by reaction with garnet and cordierite (Pattison & Tracy, 1991):

$$\text{Bt} + \text{Grt} + \text{Crd} = \text{Opx} + \text{Hc} + \text{Kfs} + \text{melt}. \quad (9)$$

The coexistence of Opx and Hc, the persistence of 'cumulus' garnet and cordierite, and absence of texturally early biotite, in many cordierite norites, indicate that reaction (9) went to completion in these rocks. The peak-metamorphic assemblage in many of the associated Opx–Crd hornfelses (Crd + Opx + Hc + Grt + Pl + Kfs + Ilm + melt) is identical to that of the cordierite norites, and indicates that the former also experienced reaction (9). The survival of minor (possibly primary) biotite in some hornfelses may be due to increased Ti and F contents in these residual micas (Patiño Douce, 1993; Dooley & Patiño Douce, 1996).

Independent evidence supporting the occurrence of reactions (2) and (6)–(9) is provided by the fact that the P–T path linking the calculated peak regional-metamorphic conditions with the peak contact-metamorphic conditions crosses the respective equilibrium curves in the expected sequence (Fig. 7). The calculated peak contact-metamorphic conditions lie just up-T of the curve for reaction (9), supporting the view that this was the highest-grade reaction to occur in the migmatites. The low a_{H_2O} values calculated for Opx–Crd hornfelses and Crd norites are consistent with the operation of high-T, fluid-absent melting reactions such as (6)–(9). Reactions of this type are strongly implicated in the production of crustally derived granitic magmas (Clemens & Watkins, 2001).

Retrograde reactions

The relatively small modal proportions of interstitial/poikilitic minerals in the cordierite norites and Opx–Crd hornfelses suggests that much of the melt produced by reactions (5)–(9) must have escaped from the rocks; further evidence for this will be provided below. On cooling, the remaining melt crystallized mainly as Bt + Qtz + Kfs + sodic Pl. Localized back-reaction of melt with residual solid phases produced fine-grained retrograde products, e.g. Bt + Qtz by the reverse of reaction (7) and sillimanite by the reverse of reaction (6) [see also Ashworth (1976)]. In Sil–Crd hornfels Dun1, late hydration of cordierite took place by the reaction

$$\text{Crd} + H_2O = \text{And} + \text{Chl} + \text{Qtz}. \quad (10)$$

This reaction occurs at relatively low temperatures ($<570°C$).

WHOLE-ROCK GEOCHEMISTRY

Some documented anatectic migmatites evidently formed as closed systems (e.g. Dougan, 1981; group 2 of Olsen, 1982), whereas others formed as open systems, recording petrological and/or geochemical evidence of melt loss (e.g. Weber *et al.*, 1985; Barbey *et al.*, 1990; Hansen & Stuk, 1993; Nyman *et al.*, 1995; Hartel & Pattison, 1996; Kriegsman, 2001; Solar & Brown, 2001). For crustal differentiation to occur, open-system behaviour is required, with transport of substantial melt volumes on a scale of kilometres. The question of whether the partial melting of Dalradian metasediments in the Huntly area was a closed- or open-system process has yet to be resolved. The key to this question lies in the geochemical relationships between the derived diatexitic rock-types (hornfelses, Crd norites and Grt tonalites) with respect to the compositions of protoliths, restitic material and melt. In a closed system, the metapelitic hornfels schollen and diatexite matrices should, when combined in their existing proportions, be chemically equivalent to the pelitic/semipelitic protoliths. If the metapelitic schollen represent restitic material, the diatexite matrices should be correspondingly enriched in melt components. In an open system with melt loss, the metapelitic hornfels schollen and diatexite matrices would sum to a composition depleted in melt components with respect to the pelitic/semipelitic protoliths, and the diatexite matrices could themselves be restitic, at least in part (Milord *et al.*, 2001).

In principle, this problem is amenable to analysis using Harker-type bivariate plots and simple mixing calculations (e.g. Dougan, 1979; Olsen, 1982, 1983). On a Harker plot showing bulk-rock concentration of a given oxide vs silica, closed-system behaviour would generate a compositional collinearity between protoliths, hornfelses and diatexite matrices, with protolith compositions straddled by the compositions of the derivative rocks. Mildly open-system behaviour would also generate this type of pattern as long as the diatexite matrices remained enriched in melt components relative to protoliths. Strongly open-system behaviour, involving much melt loss, would also generate a collinearity, but here the hornfels and diatexite matrices would both plot to one side of the protolith field. (Some smearing of the diatexite field into relatively melt-rich and melt-poor compositions might be expected if the proportion of melt loss were highly variable.) At the other end of the lever would be the average composition of the missing melts. In reality, the compositions of successive melt batches generated by reactions (5)–(9) must have changed to some extent, and may have been modified further by crystal fractionation (Milord *et al.*, 2001; Solar & Brown, 2001), but for present purposes such effects are ignored.

Bulk compositions

Major-element concentrations in 72 metasedimentary and mafic igneous rocks were obtained by X-ray fluorescence (XRF) spectrometry. Samples were prepared as pressed boric acid pellets, each containing $2{\cdot}0 \pm 0{\cdot}05$ g of rock powder, and analysed using a Philips PW 1450 X-ray spectrometer at the University of Manchester. Details of the correction procedures used have been described by Brown *et al.* (1973). Representative analyses are presented in Table 6, and the full dataset has been listed by Dalrymple (1995).

For purposes of geochemical comparison, the rocks of metasedimentary origin are split into the following geographical groupings: (1) southern complex, including 10 schists from the Whitehills and Boyndie Bay formations, five Opx–Crd hornfelses, and six Crd norites; (2) western complex, including eight schists of the Portsoy formation, and four Crd–Kfs hornfelses and four Grt tonalites from the Cumrie–Cormalet area; (3) samples from any other location. Mafic igneous rocks from the whole complex are subdivided into the following petrographic groups: (1) olivine gabbros (10 samples); (2) biotite gabbros (11 samples); (3) micronorites (two samples). Mean analyses of mafic igneous rocks and metasediments from the southern and western parts of the complex are listed in Table 7.

Metasediments

The structural trend of country-rock schists to the south of the Huntly Complex, and the petrographic affinities of these rocks with the migmatites within the southern sector of the complex, strongly suggest that the protoliths of the latter were schists of the Whitehills and Boyndie Bay formations. This connection will be assumed in the following geochemical arguments. The identities of the protoliths of the migmatites in the Cumrie–Cormalet area are less certain. These migmatites also occur along strike from *in situ* schists of the Whitehills and Boyndie Bay formations, but the schists of the Portsoy formation that crop out nearby, across strike to the west (Fig. 2), are also possible candidates.

Data from the southern part of the complex display the following trends (Tables 6 and 7, Fig. 8):

(1) the bulk compositions of the Opx–Crd hornfelses and Crd norites are similar. (On the basis of the Student's *t* test, estimated population means for Opx–Crd hornfelses and Crd norites are statistically indistinguishable, at the 95% confidence level, for all 10 oxides listed.)

Table 6: Representative XRF bulk analyses of representative rocks from the Huntly Complex

	Mafic igneous rocks			Country rock pelitic schists				Hornfelses			Diatexite matrix rocks		
	Olivine gabbro Bin2	Biotite gabbro BQ30	Micro-norite BQ27	Mica schist Bog1	And–mica schist Clas112	Biotite schist Mike1	Grt–Bt schist Sin2	Crd–Kfs hornfels Cum2ii	Opx–Crd hornfels Dun3	Opx–Crd hornfels Pir4	Garnet tonalite Cum102	Cordierite norite Dun4	Cordierite norite CasB5
SiO_2	47·00	49·12	54·81	59·58	56·52	64·47	69·34	55·38	47·27	47·59	63·62	54·50	57·78
TiO_2	0·20	1·20	1·67	1·51	1·47	1·12	0·84	1·99	2·80	1·95	1·46	1·86	1·92
Al_2O_3	19·74	20·16	21·13	21·74	19·93	18·19	14·60	20·54	25·03	27·51	16·68	16·89	16·82
FeO_T	5·41	8·29	8·06	5·77	10·83	6·10	4·97	7·93	12·05	10·69	6·40	10·13	9·19
MnO	0·19	0·20	0·08	0·16	0·18	0·18	0·00	0·17	0·18	0·20	0·16	0·07	0·32
MgO	14·05	7·73	2·84	2·29	2·97	1·39	3·93	3·12	7·07	4·27	2·41	8·21	6·99
CaO	10·22	9·80	6·59	0·98	0·95	0·89	0·74	2·94	1·97	2·85	1·96	3·86	2·06
Na_2O	2·54	2·60	4·24	2·28	1·45	3·79	2·38	4·81	1·93	3·62	3·40	2·36	1·90
K_2O	0·63	0·73	0·54	5·44	5·38	3·70	3·11	2·94	1·60	1·28	3·88	1·73	2·94
P_2O_5	0·02	0·17	0·04	0·25	0·32	0·17	0·09	0·18	0·10	0·04	0·03	0·39	0·08
Total	100·00	100·00	100·00	100·00	100·00	100·00	100·00	100·00	100·00	100·00	100·00	100·00	100·00

Major-element oxide wt % normalized to anhydrous totals of 100%. All Fe calculated as FeO.

Table 7: Mean major-element compositions of rocks of the Huntly Complex and its schist envelope

	Metasediments: southern part of complex			Metasediments: western part of complex			Gabbros	
	Schists ($n = 12$)	Opx–Crd hfls ($n = 5$)	Crd norites* ($n = 8$)	Schists ($n = 8$)	Crd–Kfs hfls ($n = 4$)	Grt tonalites ($n = 4$)	Ol gabbros ($n = 10$)	Bt gabbros ($n = 11$)
SiO_2	63·73 (5·40)	50·06 (4·96)	52·43 (5·01)	66·42 (7·50)	54·98 (1·23)	61·55 (2·69)	48·01 (2·42)	51·10 (2·74)
TiO_2	1·35 (0·31)	2·02 (0·37)	1·84 (0·62)	0·90 (0·24)	1·72 (0·46)	1·53 (0·09)	0·27 (0·22)	1·63 (0·55)
Al_2O_3	17·69 (3·60)	22·51 (4·90)	20·65 (3·52)	15·73 (4·95)	17·69 (3·48)	17·38 (1·09)	19·25 (2·17)	17·74 (1·88)
FeO_T	7·14 (1·85)	11·30 (1·83)	11·02 (2·18)	6·26 (2·02)	11·16 (2·35)	7·41 (1·76)	5·82 (1·22)	8·79 (0·93)
MnO	0·18 (0·07)	0·37 (0·30)	0·19 (0·08)	0·14 (0·07)	0·23 (0·05)	0·17 (0·01)	0·19 (0·03)	0·22 (0·02)
MgO	2·17 (0·45)	4·68 (1·90)	6·65 (2·47)	4·81 (1·35)	3·94 (1·87)	2·63 (0·30)	12·40 (2·98)	7·32 (1·57)
CaO	1·48 (1·69)	3·46 (1·31)	2·26 (1·04)	0·68 (0·34)	3·82 (1·11)	2·12 (1·35)	11·18 (1·49)	8·89 (1·62)
Na_2O	1·82 (1·12)	3·75 (1·56)	2·29 (0·79)	1·74 (0·86)	3·92 (0·63)	3·26 (0·13)	2·49 (0·65)	2·72 (1·09)
K_2O	4·23 (1·31)	1·69 (0·79)	2·56 (1·89)	3·21 (1·08)	2·27 (0·45)	3·81 (1·20)	0·37 (0·32)	1·32 (0·50)
P_2O_5	0·21 (0·10)	0·16 (0·18)	0·11 (0·13)	0·11 (0·03)	0·27 (0·33)	0·14 (0·13)	0·02 (0·01)	0·27 (0·18)
Total	100·00	100·00	100·00	100·00	100·00	100·00	100·00	100·00

*Includes two analyses from Read (1923*a*).
All Fe calculated as FeO. Anhydrous totals normalized to 100%. Errors (in parentheses) quoted as 1σ.

(2) The SiO_2 and K_2O contents of both Opx–Crd hornfelses and Crd norites are significantly lower than those of country-rock schists, whereas FeO_T, MgO, CaO and TiO_2 contents are higher.

(3) No oxides have significantly higher concentrations in the Opx–Crd hornfelses than in country-rock schists but lower concentrations in the Crd norites than in the schists. Similarly, no oxides have significantly lower concentrations in the Opx–Crd hornfelses than in country-rock schists but higher concentrations in the Crd norites than in the schists.

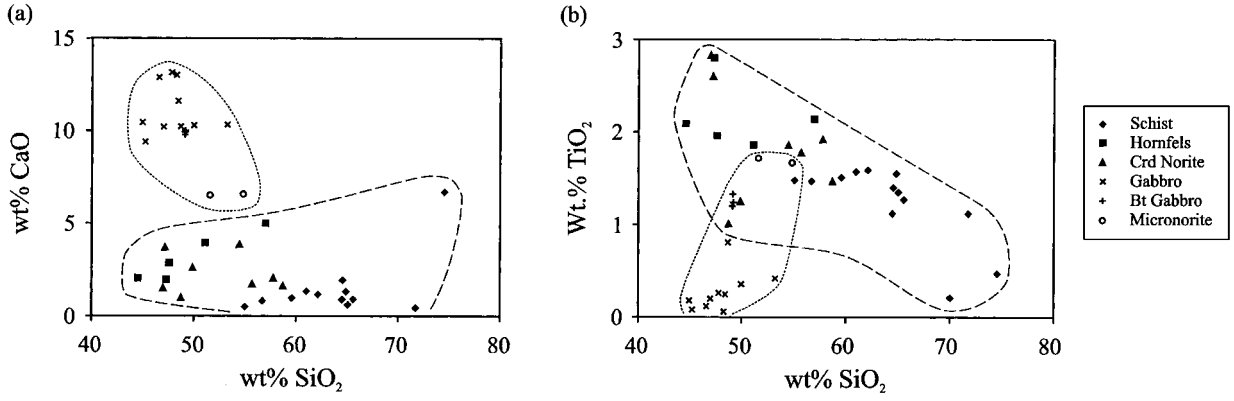

Fig. 8. Whole-rock geochemistry of rocks from the Huntly Gabbro and its southern margin. (a) CaO vs SiO_2 plot; (b) TiO_2 vs SiO_2 plot.

These findings show that the Opx–Crd hornfelses and Crd norites are depleted in 'granitophile' components relative to their likely schist protoliths and enriched in 'restitic' components. The formation of Crd norites must therefore have been an open-system process with respect to melt, and large amounts of felsic melt must have escaped.

The interpretation of the data for the western part of the complex is less clear-cut. The schists of the Portsoy formation show a much wider range of compositions but are similar, in general, to those of the Whitehills and Boyndie Bay formations, except in having higher MgO and lower CaO and TiO_2 contents (Table 7). With respect to either group of schists, the Crd–Kfs hornfelses have somewhat lower SiO_2 and higher FeO_T and CaO contents, consistent with moderate enrichment in 'restitic' components relative to protoliths. The compositions of the Grt tonalites are indistinguishable, within error, from those of either schist group, except in having higher Na_2O contents. The fact that the Grt tonalites are not significantly enriched in 'granitophile' components relative to schist protoliths (to balance, as it were, the depleted Crd–Kfs hornfelses) implies that the Grt tonalites also formed by an open-system process involving loss of felsic melt, although with smaller proportions of melt loss than in the formation of the Crd norites and Opx–Crd hornfelses.

Gabbros

For many oxides, olivine gabbro compositions are well clustered and plot far from the schist–diatexite matrix–hornfels trend on Harker diagrams. For MgO and CaO (Fig. 8a) olivine gabbros plot consistently above the trend, whereas for TiO_2 (Fig. 8b) and FeO_T they plot below. The lack of a collinearity between olivine gabbro, Crd norite and schist fields for these oxides adds further weight to the argument that the Crd norites did not form by assimilation of pelitic schist by mafic magma.

Biotite gabbros are similar in composition to olivine gabbros, except in having somewhat higher TiO_2, FeO_T and K_2O, and lower MgO and CaO (Tables 6 and 7). Being rich in biotite, a hydrous mineral, the biotite gabbros must also contain more H_2O than the olivine gabbros. However, as the SiO_2 contents of the two groups are similar, no collinearity exists between olivine gabbros, biotite gabbros and any possible siliceous 'fugitive melt' composition. Thus, the biotite gabbros could not have formed by simple mixing of siliceous melt with basic magma. However, the proximity of the biotite gabbros to contacts with metasediments coupled with their enrichment in the above components suggests that these gabbros have undergone some selective contamination, possibly by diffusion (Watson, 1982).

Mass-balance calculations

Limits on the compositions of the fugitive felsic melts can be obtained by simple linear mixing calculations, for each of the major oxides. The mean compositions of the schists and Opx–Crd hornfelses are taken as the protolith and restite compositions, respectively, for the southern sector. In mixing diagrams (Fig. 9), the melt composition is constrained to lie on the hornfels–protolith mixing lines, somewhere to the SiO_2-rich side of the protolith point. All melt components will have positive coefficients, and the closer the melt composition is to that of the protolith, the higher the proportion of extracted melt required to generate the hornfels residue.

The calculated mixing line for CaO (Fig. 9) descends to zero at ~74 wt % SiO_2, providing a maximum silica content for the fugitive melt. That of MgO, which is more tightly constrained, descends to zero at a similar

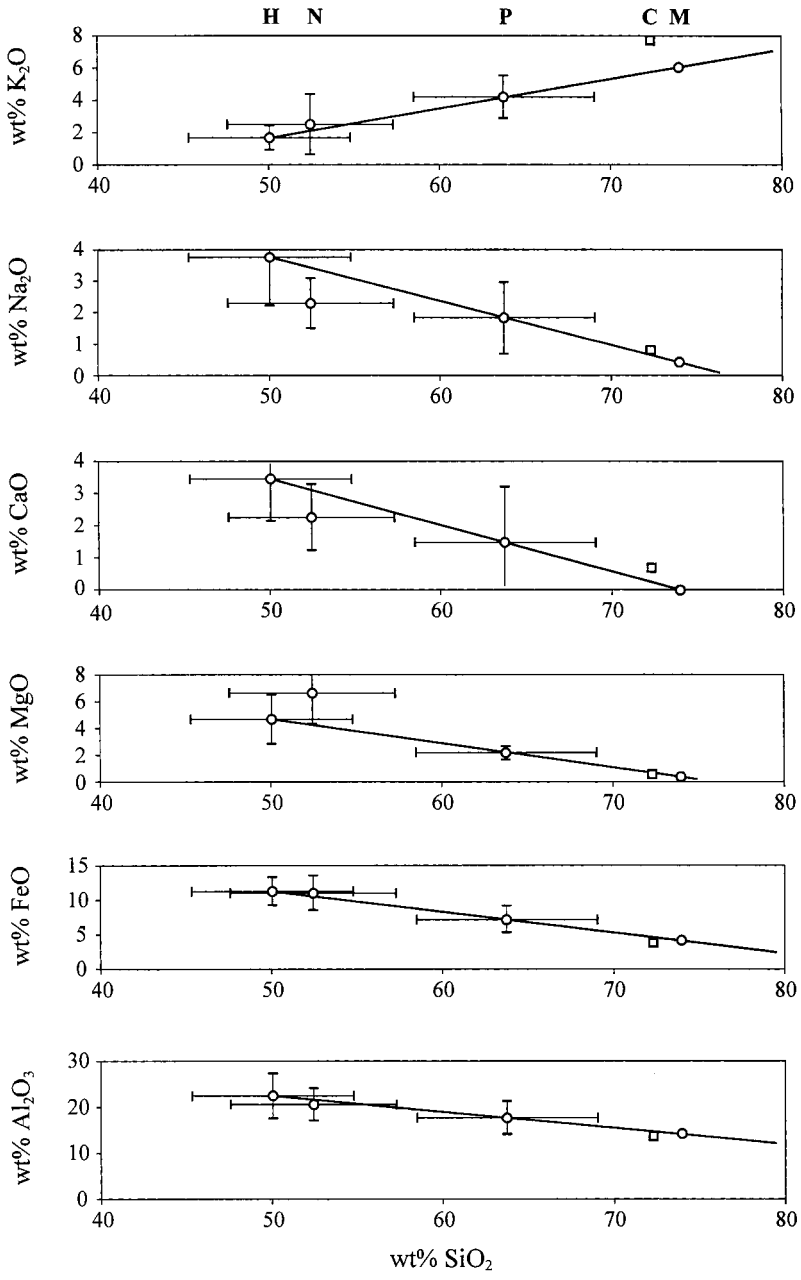

Fig. 9. Major-element mixing diagrams for rocks in the southern part of the Huntly Complex. Mean bulk compositions: H, Opx–Crd hornfelses; N, Crd norites; P, schist protoliths. Error bars are 1σ. The mixing lines are drawn through H and P. M is the most siliceous model melt composition permitted by the data (~74 wt % SiO_2). At higher silica contents the CaO content of the melt would have to be negative. The extracted melt could have a composition anywhere between P and M on the mixing lines. It should be noted that P is closer to M than to either H or N, indicating that the formation of H and N from P involved extraction of >50% m melt. C is experimental melt C112, for comparison with M.

value. The composition of the limiting CaO-free melt ('M' in Fig. 9) is broadly granitic and yields a minimum melt proportion of ~57 wt %. Table 8 shows the compositions of modelled melts that have positive, non-zero values for CaO contents. These calculations have been made for melt proportions of 60% (model melt 1) and 67% (model melt 2). Both of these model melts are peraluminous potassic granites with low normative plagioclase (<10%), high normative corundum (~7%), and Mg-number values of ~20. The calculated normative C values are similar to those of some of the experimental,

Table 8: Compositions (wt % oxide) of calculated and experimentally produced melts

	Model melt 1* 60 wt % melt S sector of complex	Model melt 2* 67 wt % melt S sector of complex	Expt'l melt C112 0·5 GPa, 900°C mean ($n = 14$)	Expt'l melt B1 0·5 GPa, 900°C mean ($n = 10$)	Expt'l melt AS 0·5 GPa, 900°C Stevens (1995)
SiO_2	72·83	70·46	72·28 (0·55)	72·35 (0·93)	74·48
TiO_2	0·90	1·01	0·39 (0·05)	0·56 (0·17)	n.a.
Al_2O_3	14·48	15·31	13·75 (0·38)	14·51 (0·67)	14·29
FeO_T	4·37	5·09	3·80 (0·16)	3·38 (0·36)	1·65
MnO	0·05	0·09	0·00 (0·00)	0·00 (0·00)	n.d.
MgO	0·50	0·94	0·55 (0·17)	0·47 (0·24)	0·25
CaO	0·17	0·51	0·69 (0·04)	1·23 (0·06)	0·64
Na_2O	0·53	0·87	0·81 (0·08)	1·47 (0·13)	2·30
K_2O	5·92	5·48	7·73 (0·12)	6·03 (0·13)	6·39
Total	99·75	99·76	100·00	100·00	100·00
CIPW norm					
Q	42·95	38·35	32·77 (0·89)	34·94 (0·97)	33·53
C	6·89	7·02	2·79 (0·51)	3·33 (0·88)	2·43
Or	34·99	32·39	45·69 (0·73)	35·64 (0·77)	37·75
Ab	4·49	7·36	6·87 (0·73)	12·46 (1·11)	19·46
An	0·84	2·53	3·43 (0·23)	6·10 (0·29)	3·18
Hy	7·88	10·19	7·71 (0·70)	6·45 (1·07)	3·65
Il	1·71	1·92	0·74 (0·10)	1·08 (0·32)	—
Total	99·75	99·76	100·00	100·00	100·00
Mg-no.	17	25	21	20	21

*All Fe recalculated to FeO.

alumina-saturated melts reported by Gardien *et al.* (1995) but somewhat higher than those reported by other workers (e.g. Clemens & Wall, 1981). The minimum proportion of model melt 1 that would have to be extracted from the schist protolith, to generate a Crd norite with the same SiO_2 content as the observed mean (52·43 wt %), is 53 wt %.

The results of these mass-balance calculations confirm that the Opx–Crd hornfelses and Crd norites of the southern part of the Huntly Complex are extremely restitic in character and require that large proportions ($> \sim$57 wt % and $> \sim$53 wt %, respectively) of the material that originally constituted the protoliths must have escaped from these rocks as magma. In this respect, the Crd norites resemble the garnet-rich diatexites described by Barbey *et al.* (1990), although the amounts of melt loss from the former were even higher. In theory, the fugitive melt could have had an SiO_2 content anywhere in the range 64–74%, but a value close to the upper end of this spectrum (corresponding to a granite) seems most likely. The reasons for this inference are that (1) this composition would minimize the amount of melt that would have to have been extracted, and (2) this is the kind of melt composition that is produced when metapelites are subjected experimentally to P–T conditions similar to those inferred for the Opx-bearing diatexites. The melt produced by Stevens (1995) from an aluminous metapelite protolith at 0·5 GPa and 900°C is similar to model melt 1, except in having higher normative plagioclase and lower normative C and Hy (Table 8). If the fugitive melts were granitoid (i.e. with 72–75 wt % SiO_2) and if, as seems likely on petrographic grounds, many of the Opx–Crd hornfelses were completely or almost completely drained of melt during their formation, then 60% seems a reasonable estimate of the degree of partial melting. The slightly lower proportion of melt loss calculated for the Crd norites is consistent with the petrographic evidence for retention of some melt during the crystallization of these rocks (namely, sub/euhedral growth of restitic phases, interstitial quartz and K-rich phases with small

dihedral angles, and igneous-type zoning patterns in plagioclase rims).

EXPERIMENTS

Partial melting experiments were undertaken, on two samples of country-rock schist from the southern margin of the Huntly Complex, to provide independent evidence of the nature and quantity of melt that could have been produced in these protoliths at the inferred P–T conditions of contact metamorphism, and the identities and compositions of coexisting minerals.

Experimental details and melt analysis

The rocks chosen as starting materials were Clas112 and Bog1 (see Table 1 for mineralogy, Table 2 for mineral compositions, and Table 6 for bulk compositions). The mineral modes of the two samples are: for Clas112: 23% Ms, 31% Bt, 24% Qtz, 10% And, 11% Pl, <1% Grt + St + Ilm; for Bog1: 26% Ms, 29% Bt, 35% Qtz, 8% Pl, 2% Tur + Ilm. Bulk H_2O contents, determined by thermogravimetry, are 2·62 (Clas112) and 2·97 wt % (Bog1).

Rock powders were prepared by grinding, in an agate ball mill, under acetone, to an average grain size of ~1 μm. Aliquots of oven-dried (110°C) powder were sealed into gold capsules and run for 150 h, without added water, in a Holloway-type internally heated argon gas vessel (Ulmer, 1971) at 0·5 GPa and 900°C. A Pd–Ag hydrogen diffusion membrane was used to impose a $\log f_{H_2} = -1$ relative to the quartz–fayalite–magnetite (QFM) buffer at nominal $a_{H_2O} = 0{\cdot}35$, to prevent loss of H_2 through the capsules (Stevens *et al.*, 1997). Pressure was measured by a manganin cell and bridge, believed to be accurate to ±10 MPa. Temperature was controlled to ±1°C and measured by type-K thermocouples, believed to be accurate to ±<5°C.

Run products were observed and analysed by EDS using a Jeol JSM 6400 scanning electron microscope. The detector system and analytical conditions were as for electron microprobe analysis. To prevent alkali loss during analysis of the glasses, the samples were cooled to –193°C by liquid nitrogen on a cryostage. Mean analyses of glasses (quenched melts) and representative analyses of minerals are listed in Tables 8 and 9, respectively.

Table 9: Representative scanning electron microscope analyses of minerals produced in partial melting experiments at 900°C and 0·5 GPa

	C112 Opx	C112 Crd	C112 Hc	C112 Bt	B1 Crd
SiO_2	45·64	48·66	0·23	34·39	49·02
TiO_2	0·36	0·00	1·04	6·30	0·00
Al_2O_3	11·04	33·91	44·12	16·36	33·53
Cr_2O_3	0·00	0·00	0·00	0·00	0·00
Fe_2O_3	—	—	10·37	—	—
FeO	26·72	6·46	31·38	20·32	7·70
MnO	0·44	0·00	0·00	0·00	0·00
MgO	15·50	10·17	4·16	8·43	9·11
CaO	0·16	0·18	0·00	0·00	0·20
Na_2O	0·41	0·00	0·00	0·41	0·30
K_2O	0·18	0·67	0·14	9·68	0·53
Total	100·44	100·04	91·44	95·89	100·41
Formula	6(O)	18(O)	4(O)	22(O)	18(O)
Si	1·73	4·90	0·01	5·27	4·95
Ti	0·01	0·00	0·02	0·73	0·00
Al	0·50	4·02	1·67	2·96	3·99
Cr	0·00	0·00	0·00	0·00	0·00
Fe^{3+}	—	—	0·25	—	—
Fe^{2+}	0·85	0·54	0·84	2·60	0·65
Mn	0·01	0·00	0·00	0·00	0·00
Mg	0·88	1·53	0·20	1·93	1·37
Ca	0·01	0·02	0·00	0·00	0·02
Na	0·03	0·00	0·00	0·12	0·06
K	0·01	0·09	0·01	1·89	0·07
Total	4·03	11·10	3·00	15·50	11·11

n.a., not analysed. C112, starting material Clas112; B1, starting material Bog1.

Experimental results

Crystalline phases

The product of the Clas112 run (C112) contains abundant small crystals of Opx, Crd, Hc, Ilm and minor Bt, suspended in a matrix of glass (Fig. 10). The Opx forms euhedral prisms up to 50 μm × 15 μm, with numerous inclusions of Ilm and Hc, and has Mg-number of 50–53 and X_{Al}^{M1} of 0·18–0·25. Cordierite forms euhedral hexagonal prisms, up to 15 μm long and 10 μm across, with Mg-number ranging from 63 to 74. Biotite forms rare ragged flakes up to 8 μm long, with 0·63–0·74 a.p.f.u. of Ti and Mg-number of 41–46. The biotite in the starting material has only 0·27–0·32 a.p.f.u. of Ti and is also more aluminous and less magnesian (Table 2). These characteristics show that the experimental biotite is a run product and, in that sense, restitic. The hercynite forms small octahedra, mostly 1–2 μm across but occasionally larger, with Mg-number of ~20. Ilmenite forms rounded granules <2 μm in diameter. Quartz and feldspar appear to be completely absent. The tight

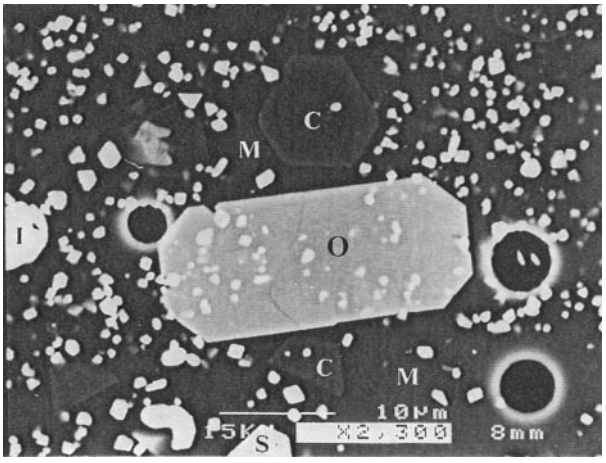

Fig. 10. Backscattered electron image from experimental run C112. Phases present include orthopyroxene (O), cordierite (C), hercynitic spinel (S), ilmenite (I) and glass (M). The three circular features are air bubbles.

clustering of compositions within C112 confirms a close approach to chemical equilibrium. The Bog1 run product (B1) contains Crd (Mg-number = 64–73), Hc, Ilm and glass. Grain sizes are smaller than in C112 but textures are similar.

The melt phase

Analysis of images (three low-magnification images per run) indicates that the volume proportion of glass in C112 lies between 55 and 65%; the overall proportion is ~60 vol. %. In B1, crystal-rich areas contain a minimum of 55 vol. % glass, whereas more typical areas contain 70 vol. %; the overall proportion is probably at least 65 vol. %. These proportions correspond closely to those reported by Gardien *et al.* (1995) for experimental melting of two-mica schist at T ~950°C.

The glass composition for each run is remarkably uniform, again confirming a close approach to equilibrium. Mean analyses of glasses in C112 and B1 (Table 8) are similar to one another and correspond to peraluminous potassic granite. The peraluminosities of the melts (~2·8 and 3·3% normative C for C112 and B1, respectively) compare well with those of other granitic melts produced experimentally in pelitic systems (e.g. Clemens & Wall, 1981; Patiño Douce & Johnston, 1991; Holtz *et al.*, 1992; Carrington & Harley, 1995; Stevens, 1995).

Comparison with natural data

Except for a lack of garnet, the FMAS mineral assemblage of C112 is similar to the non-interstitial (i.e. peak-T) mineral assemblage of the Opx–Crd hornfelses and Crd norites. The assemblage of B1 lacks orthopyroxene and is a less good match. The coexistence of Opx, Hc and melt, and lack of garnet, in C112 is evidence that reaction (9) was crossed during the experiment, and confirms that the equilibrium curve for reaction (9) lies down-temperature of the peak P–T conditions experienced by the highest-grade rocks. The apparent lack of quartz and K-feldspar and paucity of biotite in both runs is consistent with the conclusion that, in the Crd norites, these phases crystallized mainly from interstitial melt during cooling. The apparent absence of plagioclase from the runs is at variance with the deduction that plagioclase is a major constituent of the residual assemblage in both Opx–Crd hornfelses and Crd norites, but the fact that Na concentrations are lower in the glasses than in the corresponding starting rocks implies that some undetected plagioclase was indeed produced in both runs.

Minerals in C112 have compositions similar to those in the high-grade rocks. Measured Mg-number values generally fall within the ranges observed for respective minerals in Opx-bearing rocks, except for biotite, which is slightly less magnesian in C112. Ti and Al contents of C112 biotites are similar to those of Crd norites. Al contents of C112 orthopyroxenes are somewhat higher than their natural counterparts, but no more scattered.

The compositions of experimentally produced melts correspond closely to that of model melt 1 with respect to SiO_2, Al_2O_3, FeO, MgO, K_2O and Mg-number, but have slightly higher Na_2O and CaO contents and lower TiO_2 (Table 8). The match is closer than with the composition of Stevens (1995). Normative Q and C are lower than in model melt 1, normative feldspar components higher. Assuming that volume and mass proportions are not radically different, the amount of melt in the experimental runs (60–65 vol. %) agrees well with the calculated degree of partial melting (60 wt %). Collectively, these results support the findings of the thermobarometry and mass-balance calculations.

DISCUSSION

Our results show that the highest-grade pelitic rocks of the Huntly Complex underwent high degrees of anatexis (~60%), to produce strongly peraluminous, low-Ca, potassic granitic melts, as a result of the mid-crustal intrusion of mafic magma. The close correspondence between the compositions of model and experimental melts implies that little or no fractional crystallization affected the melts before their expulsion. The conclusion that these granitic melts were able to segregate efficiently from the solid products of the melting reactions, but did not mix mechanically with the mafic magma to any great extent, suggests that no

great melt pool of felsic magma actually developed above the gabbro intrusion (compare Huppert & Sparks, 1988) and that the melt was rapidly and efficiently evacuated (e.g. Sleep, 1988; Clemens & Mawer, 1992; Harris *et al.*, 2000). This raises three questions: (1) How did the fugitive melts segregate from their restitic solids? (2) Where did they go? (3) What sort of geometric relationships prevented interactions between the felsic and mafic melts?

Melt segregation

Melt segregation mechanisms in migmatites have been discussed by many workers (e.g. McKenzie, 1987; D'Lemos *et al.*, 1992; Brown, 1994; Sawyer, 1994; Brown *et al.*, 1995*a*, 1995*b*). Brown *et al.* (1995*b*) identified three principal driving forces: (1) forces arising from expansion associated with fluid-absent melting; (2) gravity-induced compaction of solids; (3) deviatoric stress-induced compaction of solids. In the diatexites of the Huntly Complex, expansion forces, although probably important in 'hydrofracturing' the rocks and segregation of melts into fractures in the initial stages of melting, are unlikely to have played the dominant role in the expulsion of anatectic melts from restitic solids, because the proportions of melt extracted were much larger than the likely proportional volume increase of fluid-absent melting. We now consider the relevance of the remaining two processes to the Huntly diatexites.

Gravity-driven compaction of solids

This process encompasses two distinct mechanisms, depending on whether the melt proportion exceeds some threshold value, usually referred to as the 'melt escape threshold' (MET) (Vigneresse *et al.*, 1996). Estimates of the MET range from 20% to 50% (e.g. van der Molen & Paterson, 1979; Rutter & Neumann, 1995). Below the MET, the solid grains form a contiguous framework, and compaction involves upward percolation of melt by porous flow through a solid matrix of finite bulk viscosity, as modelled by McKenzie (1984, 1985). For this mechanism to operate, the melt must occupy a large enough volume proportion to form an interconnected porosity, i.e. to exceed the 'liquid percolation threshold' (LPT). Above the MET, the solid grains are suspended in melt, and compaction occurs in response to the buoyancy forces acting on individual grains (i.e. by gravitational settling or floating).

Gravitational settling can be an efficient segregation mechanism provided there is a sufficiently large density contrast between solids and liquid and the liquid has a sufficiently low viscosity (Shaw, 1965). It has been shown that siliceous (granitic *sensu lato*) melts, although they have relatively high viscosities, are only one to three orders of magnitude more viscous than typical basalt melts (e.g. Scaillet *et al.*, 1998; Clemens & Petford, 1999). Thus, granitic melt viscosity is sufficiently low to permit settling of relatively dense solids (such as pyroxene, garnet and plagioclase). For this mechanism to operate in diatexites, all the melt produced on heating must remain in contact with the restitic solids until the MET is greatly exceeded. This clearly did not happen in the Huntly Opx–Crd hornfelses, as these rocks evidently retained their integrity during melting, but it could have been important in the diatexite matrices. To test the feasibility of settling in the present case, composition C112 (Table 8) was used to model the physical properties of the anatectic granitic melt, assuming a melt H_2O content of 4·5 wt %. The method of Bottinga & Weill (1970) and data of Mo *et al.* (1982) yield a density of 2240 kg/m^3 at 900°C and 0·45 GPa. The calculated viscosity (Hess & Dingwell, 1996) of C112 at 900°C is ~16 200 Pa s. Comparison of the densities of the restitic Grt, Opx, Crd and Pl in the diatexites (4080, 3600, 2580 and 2700 kg/m^3, respectively) with that of melt indicates that all restitic minerals should settle out of such a melt. Application of Stokes' Law for 2 mm diameter crystals of Grt, Opx, Crd and Pl yields settling velocities of 7·6, 5·6, 1·4 and 1·9 m/a, respectively, at 900°C. At 800°C, the velocities are an order of magnitude lower. These results suggest that restitic cumulates could form in moderate-sized (< 1 km diameter) masses of partially molten metapelite on a time-scale that is extremely short in comparison with that of the crystallization of a large gabbro intrusion. However, as the various cumulus minerals would settle at very different rates, dramatic gradations in their relative modes would be expected, unless aggregates of unlike crystals settled together. The absence of compelling field or textural evidence for layering in the Huntly diatexite matrices suggests that settling was not a major segregation mechanism.

Where crystals form a contiguous framework, Stokesian settling cannot operate, and compaction has to occur by a different mechanism. Gravity-driven compaction of a contiguous solid framework requires a relatively impermeable lower boundary, which, in the Huntly Complex, could have been provided by gabbro chilled margins against the screens and pendants of metapelite. In principle, this process might have been responsible for melt segregation from hornfelses and from diatexite matrices. Mecklenburgh (2000) used the equations of McKenzie (1984, 1985) to calculate the time taken to extract granitic melts of varying H_2O contents and temperatures by gravity-driven compaction. He showed that, where heat flow is not rate-limiting, extraction of 10% of a melt containing ~4·5 wt % H_2O at 900°C by porous flow through a

solid framework with a grain size of 5 mm would take >1·0 Myr. This is long in comparison with the time taken for a large gabbro intrusion to crystallize. However, Mecklenburgh (2000) also showed that, if an array of 5 cm wide fractures is introduced, the time taken would decrease to <100 a, which would easily be short enough to drain the diatexites of anatectic melt. No field evidence for such fracture arrays has been found in the diatexites.

Deviatoric stress-induced compaction

The existence of a far-field deviatoric stress can, in principle, cause melt segregation in systems with melt fractions between LPT and MET. As deviatoric stress can be transmitted through a contiguous solid framework of mineral grains but not through the intergranular melt, the framework can undergo strain (e.g. by diffusion-accommodated granular flow; Rutter, 1997). Provided that channels (fractures or less compacted regions) exist, the resulting stress gradient can cause expulsion of melt from the intergranular pores into the channels (Rutter & Neumann, 1995; Simakin & Talbot, 2001). Mecklenburgh (2000) used the model of Rutter & Neumann (1995) to assess the feasibility of extracting granitic melt by this mechanism; his results suggest that the time taken to extract 10% of granitic melt containing ~4·5 wt % H_2O at 900°C, from a solid framework of grain size 5 mm, into a channel network with a 2 m spacing under a constant mean effective stress of 1 MPa is ~2 kyr. In the context of the Huntly Complex, where anatexis was not accompanied by tectonism, the only far-field deviatoric stresses that could have acted on bodies of partially melted metapelite would have been those imparted by the weight of overlying lobes of the gabbro intrusion (i.e. σ_1 was vertical). Once solidified, individual gabbro lobes may have been rigid enough to sink *en masse* through their subjacent migmatites. To exert a vertical stress of 1 MPa on its substrate, a slab of gabbro of density 3000 kg/m^3 would only need to be ~0·5 km thick, if surrounded by partially melted metapelite of density 2800 kg/m^3 (30% granitic melt and 70% restite). For this stress to have caused segregation, however, a contiguous solid framework must have extended from the floor to the roof of the partially melted metapelite substrate. One way in which such a framework could have been maintained could be that the melt was extracted continually, as it was produced, thus keeping the melt fraction low throughout the melting history, as advocated by Sawyer (1994).

Fate of the fugitive melts

The anatectic melts of the Huntly Complex were generated under conditions favourable to their migration to higher and cooler levels of the crust. The high temperature of the melts and their H_2O-undersaturated compositions are both factors that would have facilitated melt ascent (Brown & Fyfe, 1970; Stevens & Clemens, 1993). The sizes of individual coalesced melt bodies is also a factor. The larger the melt body the larger is its 'thermal inertia' during ascent into cold crust. In the absence of good geological control on the 3D shapes of the gabbro and diatexite bodies of the Huntly Complex, neither the total anatectic melt volume nor the volumes of individual melt bodies can be estimated with confidence. Nevertheless, crude estimates of melt volume can be made for individual migmatite bodies assuming that they are equant in 3D and have outcrop areas as in Fig. 2. The most restitic diatexites are those in the south of the complex. Some of these (e.g. NE of the Deveron near Dunbennan Hill) have outcrops ~300 m in diameter, yielding a restite volume of ~0·015 km^3. Assuming a conservative melt fraction of 50%, the local melt volume was also 0·015 km^3. The cluster of exposures near the Deveron, north of Huntly, may belong to a single outcrop ~1 km across, which would yield a melt volume of ~0·5 km^3. (The Cumrie–Cormalet outcrop is even larger but has evidently undergone less melt depletion.) Once segregated, such volumes of melt would have been large enough to rise considerable distances through pre-warmed Dalradian country rocks before crystallizing, probably utilizing interconnected fractures, as advocated by Clemens & Mawer (1992) and described by Johnson *et al.* (2001*b*).

The equations of Petford *et al.* (1993, 1994) can be used to estimate the minimum width of fractures required to prevent solidification of the rising magma by freezing. Assuming a magma temperature of 900°C, a magma solidus temperature of 750°C, a far-field temperature of 540°C, a latent heat of fusion of 3×10^5 J/kg, a specific heat capacity of 1200 J/kg/°C, a thermal diffusivity of 8×10^{-7} m^2/s, a density difference between country rock and magma of 560 kg/m^3, and a magma viscosity of 16 000 Pa s, the critical width of a fracture of height 1 km is estimated to be ~0·4 m. This implies that any fractures wider than ~0·4 m should have been able to act as magma conduits, and any narrower than this should have frozen to form dykes. For a height of 5 km, the estimated critical width is ~0·55 m. Peraluminous aplite and leucogranite sheets, some ~1 m thick, which may represent such conduits, occur in the relatively high-grade but unmigmatized parts of the Buchan terrane (Johnson *et al.*, 2000).

Regarding potential sinks for the fugitive melts, numerous S-type granites occur in the Buchan region east of the Huntly Complex (and at higher structural levels), as both minor (Johnson *et al.*, 2000, 2001*b*) and major (Brown, 1991) intrusions. Many of these (e.g.

Strichen, Aberchirder) belong to the contemporaneous, Grampian suite of peraluminous two-mica granites. The latter have isotopic signatures implying an upper-crustal source (Harmon, 1983). We have shown that the fugitive melts from the Huntly Complex were also peraluminous and granitic, suggesting that they may have contributed to the Grampian suite. Anatectic melts were probably also supplied from the other Newer Gabbro and related mafic complexes (e.g. Johnson *et al.*, 2001*b*).

A significant implication of this work is that crustal fusion and magma production can occur without significant chemical interaction between the mantle-derived heat source and the crustal melts. This is important because it explains how 'pure' S-type magmas might arise.

CONCLUSIONS

(1) Syn-metamorphic intrusion of mafic magma into warm (~550°C) Dalradian metapelites and semipelites at mid-crustal depths in the Huntly area, NE Scotland, resulted locally in peak-metamorphic temperatures of ~900°C, and in high degrees of partial melting via incongruent, fluid-absent, melting reactions.

(2) The anatectic melts were of H_2O-undersaturated, peraluminous, low-Ca, potassic granite composition. In many places, a large proportion of the melt escaped from the sites of generation. The melts underwent little or no *in situ* fractional crystallization before escaping.

(3) Segregation of melts from restites was probably achieved by purely gravitational processes, and appears not to have required regional tectonic deviatoric stresses. The role of transient fracture formation was probably critical to various stages of the segregation process.

(4) The fugitive granitic melts did not mix significantly with the gabbroic magma, although some selective contamination of the mafic magma may have occurred, leading to the generation of biotite gabbros. The bulk of the melt escaped and probably contributed to the Grampian suite of S-type granites in this region. Thus, crustal fusion and magma production can occur without significant chemical interaction between the mantle-derived heat source and the crustal melts.

(5) Opx–Crd hornfels xenoliths represent solid Ca-, Mg-, Fe-, Al-, Na-rich residues left after extraction of ~60% melt. The Crd norite diatexite matrix rocks are also residual, and represent restite-enriched crystal–liquid mushes left after extraction of ~55% melt. Grt tonalites probably also represent restite-enriched mushes, but retaining a higher proportion of residual melt than the Crd norites.

(6) The mid-Ordovician middle crust of NE Scotland was the site of localized crustal differentiation in response to intrusion of large volumes of mantle-derived mafic magma.

(7) The prograde P–T path of contact-metamorphic rocks in the SW part of the Huntly Complex had a low positive dP/dT slope, indicating that the gabbro intrusion itself increased the lithostatic load on the country rocks.

ACKNOWLEDGEMENTS

This paper is derived from the Ph.D. thesis of D.J.D., supervised at Manchester by G.T.R.D. and J.D.C. The work was supported by an NERC research studentship, which is gratefully acknowledged. We thank D. Plant, P. Lythgoe, S. Caldwell and C. Davies for technical support. Tracy Rushmer, Marion Holness and an anonymous referee are thanked for their helpful comments.

REFERENCES

Allan, W. C. (1970). The Morven–Cabrach basic intrusion. *Scottish Journal of Geology* **6**, 53–72.

Ashcroft, W. A. & Boyd, R. (1976). The Belhelvie mafic igneous intrusion, Aberdeenshire—a reinvestigation. *Scottish Journal of Geology* **12**, 1–14.

Ashcroft, W. A. & Munro, M. (1978). The structure of the eastern part of the Insch mafic intrusion, Aberdeenshire. *Scottish Journal of Geology* **14**, 55–79.

Ashcroft, W. A., Kneller, B. C., Leslie, A. G. & Munro, M. (1984). Major shear zones and allochthonous Dalradian in the north-east Scottish Dalradian. *Nature* **310**, 760–762.

Ashworth, J. R. (1975). The sillimanite zones of the Huntly–Portsoy area in the north-east Dalradian, Scotland. *Geological Magazine* **112**, 113–136.

Ashworth, J. R. (1976). Petrogenesis of migmatites in the Huntly–Portsoy area, north-east Scotland. *Mineralogical Magazine* **40**, 661–682.

Ashworth, J. R. (1985). Introduction. In: Ashworth, J. R. (ed.) *Migmatites*. Glasgow: Blackie, pp. 1–35.

Ashworth, J. R. & Chinner, G. A. (1978). Coexisting garnet and cordierite in migmatites from the Scottish Caledonides. *Contributions to Mineralogy and Petrology* **65**, 379–394.

Baker, A. J. (1987). Models for the tectonothermal evolution of the eastern Dalradian of Scotland. *Journal of Metamorphic Geology* **5**, 101–118.

Barbey, P., Macaudiere, J. & Nzenti, J. P. (1990). High-pressure dehydration melting of metapelites: evidence from the migmatites of Yaoundé (Cameroon). *Journal of Petrology* **31**, 401–428.

Beddoe-Stephens, B. (1990). Pressures and temperatures of Dalradian metamorphism and the andalusite–kyanite transformation in the northeast Grampians. *Scottish Journal of Geology* **26**, 3–14.

Berman, R. G. (1990). Mixing properties of Ca–Mg–Fe–Mn garnets. *American Mineralogist* **75**, 328–344.

Bhattacharya, A., Krishnakumar, K., Raith, M. & Sen, S. K. (1991). An improved set of a–X parameters for pyrope–almandine binary garnets and refinement of the orthopyroxene–garnet

thermometer and orthopyroxene–garnet–plagioclase–quartz barometer. *Journal of Petrology* **32**, 629–656.

Bhattacharya, A., Mohanty, L., Maji, A., Sen, S. K. & Raith, M. (1992). Non-ideal mixing in the phlogopite–annite binary: constraints from experimental data on Mg–Fe partitioning and a reformulation of the biotite–garnet geothermometer. *Contributions to Mineralogy and Petrology* **109**, 107–111.

Bottinga, Y. & Weill, D. F. (1970). Densities of liquid silicate systems calculated from partial molar volumes of oxide components. *American Journal of Science* **269**, 169–182.

Boyd, R. & Munro, M. (1978). Deformation of the Belhelvie mass, Aberdeenshire. *Scottish Journal of Geology* **14**, 29–44.

Brown, G. C. & Fyfe, W. S. (1970). The production of granitic melts during ultrametamorphism. *Contributions to Mineralogy and Petrology* **28**, 310–318.

Brown, G. C., Hughes, D. J. & Esson, J. (1973). New XRF data retrieval techniques and their application to USGS standard rocks. *Chemical Geology* **11**, 223–229.

Brown, M. (1994). The generation, segregation, ascent and emplacement of granitic magma: the migmatite-to-crustally-derived granite connection in thickened orogens. *Earth-Science Reviews* **36**, 83–130.

Brown, M., Averkin, Y. A. & McLennan, E. L. (1995*a*). Melt segregation in migmatites. *Journal of Geophysical Research* **100**, 15665–15679.

Brown, M., Rushmer, T. & Sawyer, E. W. (1995*b*). Introduction to special section: mechanisms and consequences of melt segregation from crustal protoliths. *Journal of Geophysical Research* **100**, 15551–15563.

Brown, P. E. (1991). Caledonian and earlier magmatism. In: Craig, G. Y. (ed.) *Geology of Scotland*. London: Geological Society, pp. 229–295.

Carrington, D. P. & Harley, S. L. (1995). Partial melting and phase relations in high-grade metapelites—an experimental petrogenetic grid in the KFMASH system. *Contributions to Mineralogy and Petrology* **120**, 270–291.

Carrington, D. P. & Harley, S. L. (1996). Cordierite as a monitor of fluid and melt water contents in the lower crust: an experimental calibration. *Geology* **24**, 647–650.

Chatterjee, N. D. & Flux, S. (1986). Thermodynamic mixing properties of muscovite–paragonite crystalline solutions at high temperatures and pressures, and their geological applications. *Journal of Petrology* **27**, 677–693.

Chinner, G. A. (1966). The distribution of pressure and temperature during Dalradian metamorphism. *Journal of the Geological Society, London* **122**, 159–186.

Chinner, G. A. (1980). Kyanite isograds of Grampian metamorphism. *Journal of the Geological Society, London* **137**, 35–39.

Chinner, G. A. & Heseltine, F. J. (1979). The Grampide andalusite/kyanite isograd. *Scottish Journal of Geology* **15**, 81–168.

Chinner, G. A. & Schairer, J. F. (1962). The join $Ca_3Al_2Si_3O_{12}$–$Mg_3Al_2Si_3O_{12}$ and its bearing on the system CaO–MgO–Al_2O_3–SiO_2 at atmospheric pressure. *American Journal of Science* **260**, 611–634.

Clarke, P. D. & Wadsworth, W. J. (1970). The Insch layered intrusion. *Scottish Journal of Geology* **6**, 7–25.

Clemens, J. D. (1990). The granulite granite connexion. In: Vielzeuf, D. & Vidal, P. (eds) *Granulites and Crustal Differentiation*. Dordrecht: Kluwer Academic, pp. 25–36.

Clemens, J. D. & Droop, G. T. R. (1998). Fluids, *P–T* paths and the fates of anatectic melts in the Earth's crust. *Lithos* **44**, 21–36.

Clemens, J. D. & Mawer, C. K. (1992). Granitic magma transport by fracture propagation. *Tectonophysics* **204**, 339–360.

Clemens, J. D. & Petford, N. (1999). Granitic melt viscosity and silicic magma dynamics in contrasting tectonic settings. *Journal of the Geological Society, London* **156**, 1057–1060.

Clemens, J. D. & Wall, V. J. (1981). Crystallization and origin of some peraluminous (S-type) granitic magmas. *Canadian Mineralogist* **19**, 111–131.

Clemens, J. D. & Watkins, J. M. (2001). The fluid regime of high-temperature metamorphism during granitoid magma genesis. *Contributions to Mineralogy and Petrology* **140**, 600–606.

Clemens, J. D., Petford, N. & Mawer, C. K. (1997). Ascent mechanisms of granitic magmas: causes and consequences. In: Holness, M. (ed.) *Deformation-Enhanced Fluid Transport in the Earth's Crust and Mantle*. London: Chapman and Hall, pp. 144–171.

Conrad, W. K., Nicholls, I. A. & Wall, V. J. (1988). Water-saturated and -undersaturated melting of metaluminous and peraluminous crustal compositions at 10 kb: evidence for the origin of silicic magmas in the Taupo Volcanic Zone, New Zealand, and other occurrences. *Journal of Petrology* **29**, 765–803.

Dalrymple, D. J. (1995). Contact anatexis of Dalradian metapelites from the Huntly–Knock area, Aberdeenshire, N. E. Scotland. Ph.D. thesis, University of Manchester, 406 pp.

Dempster, T. J., Hudson, N. F. C. & Rogers, G. (1995). Metamorphism and cooling of the NE Dalradian. *Journal of the Geological Society, London* **152**, 431–437.

Dempster, T. J., Rogers, G., Tanner, P. W. G., Bluck, B. J., Muir, R. J., Redwood, S. D., Ireland, T. R. & Paterson, B. A. (2002). Timing of deposition, orogenesis, and glaciation within the Dalradian rocks of Scotland: constraints from U–Pb zircon ages. *Journal of the Geological Society, London* **159**, 83–94.

D'Lemos, R. S., Brown, M. & Strachan, R. A. (1992). Granite magma generation, ascent and emplacement within a transpressional orogen. *Journal of the Geological Society, London* **149**, 487–490.

Dooley, D. F. & Patiño Douce, A. (1996). Fluid-absent melting of F-rich phlogopite + rutile + quartz. *American Mineralogist* **81**, 202–212.

Dougan, T. W. (1979). Compositional and modal relationships and melting reactions in some migmatitic metapelites from New Hampshire and Maine. *American Journal of Science* **279**, 897–935.

Dougan, T. W. (1981). Melting reactions and trace element relationships in selected specimens of migmatitic metapelites from New Hampshire and Maine. *Contributions to Mineralogy and Petrology* **78**, 337–344.

Droop, G. T. R. (1987). A general equation for estimating Fe^{3+} concentrations in ferromagnesian silicates and oxides using stoichiometric criteria. *Mineralogical Magazine* **51**, 431–437.

Droop, G. T. R. & Charnley, N. R. (1985). Comparative geobarometry of pelitic hornfelses associated with the Newer Gabbros: a preliminary study. *Journal of the Geological Society, London* **142**, 53–62.

Elkins, L. T. & Grove, T. L. (1991). Ternary feldspar experiments and thermodynamic models. *American Mineralogist* **75**, 544–559.

England, P. C. & Thompson, A. B. (1986). Some thermal and tectonic models for crustal melting in continental collision zones. In: Coward, M. P. & Ries, A. C. (eds) *Collision Tectonics, Geological Society, London, Special Publications* **19**, 83–94.

Fettes, D. J. (1970). The structural and metamorphic state of the Dalradian rocks and their bearing on the age of emplacement of the basic sheet. *Scottish Journal of Geology* **6**, 108–118.

Finger, F. & Clemens, J. D. (1995). Migmatization and 'secondary' granitic magmas: effects of emplacement of 'primary' granitoids

in Southern Bohemia, Austria. *Contributions to Mineralogy and Petrology* **120**, 311–326.

Fitzsimons, I. C. W. & Harley, S. L. (1994). The influence of retrograde cation exchange on granulite *P–T* estimates and a convergence technique for the recovery of peak-metamorphic conditions. *Journal of Petrology* **35**, 543–576.

Frost, B. R. & Chacko, T. (1989). The granulite uncertainty principle: limitations on thermobarometry in granulites. *Journal of Geology* **97**, 435–450.

Gardien, V., Thompson, A. B., Grujic, D. & Ulmer, P. (1995). Experimental melting of biotite + plagioclase + quartz ± muscovite assemblages and implications for crustal melting. *Journal of Geophysical Research* **B100**, 15581–15591.

Grant, J. A. (1985*a*). Phase equilibria in low-pressure partial melting of pelitic rocks. *American Journal of Science* **285**, 409–435.

Grant, J. A. (1985*b*). Phase equilibria in partial melting of pelitic rocks. In: Ashworth, J. R. (ed.) *Migmatites*. Glasgow: Blackie, pp. 86–114.

Grant, J. A. & Frost, B. R. (1990). Contact metamorphism and partial melting of pelitic rocks in the aureole of the Laramie Anorthosite complex, Morton Pass, Wyoming. *American Journal of Science* **290**, 425–472.

Greenfield, J. E., Clarke, G. L., Bland, M. & Clark, D. C. (1996). *In situ* migmatite and hybrid diatexite at Mt. Stafford, Central Australia. *Journal of Metamorphic Geology* **14**, 413–426.

Gribble, C. D. (1966). The thermal aureole of the Haddo House norite in Aberdeenshire. *Scottish Journal of Geology* **2**, 306–313.

Gribble, C. D. (1968). The cordierite-bearing rocks of the Haddo House and Arnage districts, Aberdeenshire. *Contributions to Mineralogy and Petrology* **17**, 315–330.

Gribble, C. D. (1970). The role of partial fusion in the generation of certain cordierite-bearing rocks. *Scottish Journal of Geology* **6**, 75–82.

Gribble, C. D. & O'Hara, M. J. (1967). Interaction of basic magma and pelitic materials. *Nature* **214**, 1198–1201.

Hansen, E. & Stuk, M. (1993). Orthopyroxene-bearing mafic migmatites at Cone Peak, California: evidence for the formation of migmatitic granulites by anatexis in an open system. *Journal of Metamorphic Geology* **11**, 291–307.

Harley, S. L. & Green, D. H. (1982). Garnet–orthopyroxene barometry for granulites and peridotites. *Nature* **300**, 697–701.

Harley, S. L., Thompson, P., Hensen., B. J. & Buick, I. S. (2002). Cordierite as a sensor of fluid conditions in high-grade metamorphism and crustal anatexis. *Journal of Metamorphic Geology* **20**, 71–86.

Harmon, R. S. (1983). Oxygen and strontium isotopic evidence regarding the role of continental crust in the origin and evolution of British Caledonian granites. In: Atherton, M. P. & Gribble, C. D. (eds) *Migmatites, Melting and Metamorphism*. Nantwich: Shiva, pp. 62–79.

Harris, N. B. W., Vance, D. & Ayres, M. (2000). From sediment to granite: timescales of anatexis in the upper crust. *Chemical Geology* **162**, 155–167.

Harte, B. (1988). Lower Palaeozoic metamorphism in the Moine–Dalradian belt of the British Isles. In: Harris, A. L. & Fettes, D. J. (eds) *The Caledonian–Appalachian Orogen. Geological Society, London, Special Publications* **38**, 123–134.

Harte, B. & Hudson, N. F. C. (1979). Metapelite facies series and temperatures and pressures of Dalradian metamorphism in eastern Scotland. In: Harris, A. L., Holland, C. H. & Leake, B. E. (eds) *The Caledonides of the British Isles Reviewed. Geological Society, London, Special Publications* **8**, 323–337.

Harte, B., Pattison, D. R. M. & Linklater, C. M. (1991). Field relations and petrography of partially melted pelitic and semi-pelitic rocks. In: Voll, G., Töpel, J., Pattison, D. R. M. & Seifert, F. (eds) *Equilibrium and Kinetics in Contact Metamorphism: the Ballachulish Igneous Complex and its Aureole*. Berlin: Springer, pp. 182–210.

Hartel, T. H. D. & Pattison, D. R. M. (1996). Genesis of the Kapuskasing (Ontario) migmatitic mafic granulites by dehydration melting of amphibolite: the importance of quartz to reaction progress. *Journal of Metamorphic Geology* **14**, 591–611.

Hess, K.-U. & Dingwell, D. B. (1996). Viscosities of hydrous leucogranitic melts: a non-Arrhenian model. *American Mineralogist* **81**, 1297–1300.

Holland, T. J. B. & Powell, R. (1990). An enlarged and updated internally consistent thermodynamic dataset with uncertainties and correlations: the system Na_2O–K_2O–CaO–MgO–MnO–FeO–Fe_2O_3–Al_2O_3–SiO_2–TiO_2–C–H_2–O_2. *Journal of Metamorphic Geology* **8**, 89–124.

Holland, T. J. B. & Powell, R. (1998). An internally consistent thermodynamic dataset for phases of petrological interest. *Journal of Metamorphic Geology* **16**, 309–344.

Holness, M. B. & Clemens, J. D. (1999). Partial melting of the Appin 'Quartzite' driven by fracture-controlled H_2O infiltration in the aureole of the Ballachulish Igneous Complex, Scottish Highlands. *Contributions to Mineralogy and Petrology* **136**, 154–168.

Holland, T. J. B., Babu, E. V. S. S. K. & Waters, D. J. (1996). Phase relations of osumilite and dehydration melting in pelitic rocks: a simple thermodynamic model for the KFMASH system. *Contributions to Mineralogy and Petrology* **124**, 383–394.

Holtz, F. & Johannes, W. (1994). Maximum and minimum water contents of granitic melts: implications for chemical and physical properties of ascending magmas. *Lithos* **32**, 149–159.

Holtz, F., Johannes, W. & Pichavant, M. (1992). Peraluminous granites: the effect of alumina on melt composition and coexisting minerals. *Transactions of the Royal Society of Edinburgh* **83**, 409–416.

Hudson, N. F. C. (1980). Regional metamorphism of some Dalradian metapelites in the Buchan area, N. E. Scotland. *Contributions to Mineralogy and Petrology* **73**, 39–51.

Hudson, N. F. C. (1985). Conditions of Dalradian metamorphism in the Buchan area, NE Scotland. *Journal of the Geological Society, London* **142**, 63–76.

Huppert, H. E. & Sparks, R. S. J. (1988). The generation of granitic magmas by intrusion of basalt into continental crust. *Journal of Petrology* **29**, 599–624.

Johannes, W. & Schreyer, W. (1981). Experimental introduction of H_2O and CO_2 into Mg-cordierite. *American Journal of Science* **281**, 299–317.

Johnson, T. E., Hudson, N. F. C. & Droop, G. T. R. (2000). Wollastonite-bearing assemblages from the Dalradian at Fraserburgh, northeast Scotland, and their bearing on the emplacement of garnetiferous granitoid sheets. *Mineralogical Magazine* **64**, 1165–1176.

Johnson, T. E., Hudson, N. F. C. & Droop, G. T. R. (2001*a*). Partial melting in the Inzie Head gneisses: the role of water and a petrogenetic grid in KFMASH applicable to anatectic pelitic migmatites. *Journal of Metamorphic Geology* **19**, 99–118.

Johnson, T. E., Hudson, N. F. C. & Droop, G. T. R. (2001*b*). Melt segregation structures within the Inzie Head gneisses of the northeastern Dalradian. *Scottish Journal of Geology* **37**, 59–72.

Kenah, C. & Hollister, L. S. (1983). Anatexis in the Central Gneiss Complex, British Columbia. In: Atherton, M. P. & Gribble, C. D. (eds) *Migmatites, Melting and Metamorphism*. Nantwich: Shiva, pp. 142–162.

Kneller, B. & Aftalion, M. (1987). The isotopic and structural age of the Aberdeen Granite. *Journal of the Geological Society, London* **144**, 717–721.

Kretz, R. (1983) Symbols for rock-forming minerals. *American Mineralogist* **68**, 277–279.

Kriegsman, L. M. (2001). Partial melting, partial melt extraction and partial back reaction in anatectic migmatites. *Lithos* **56**, 75–96.

Lamb, W. M. & Valley, J. W. (1988). Granulite-facies amphibole and biotite equilibria and calculated peak-metamorphic water activities. *Contributions to Mineralogy and Petrology* **100**, 349–360.

LeBreton, N. & Thompson, A. B. (1988). Fluid-absent (dehydration) melting of biotite in metapelites in the early stages of crustal anatexis. *Contributions to Mineralogy and Petrology* **99**, 226–237.

McKenzie, D. P. (1984). The generation and compaction of partially molten rock. *Journal of Petrology* **25**, 713–765.

McKenzie, D. P. (1985). The extraction of magma from the crust and mantle. *Earth and Planetary Science Letters* **74**, 81–91.

McKenzie, D. P. (1987). The compaction of igneous and sedimentary rocks. *Journal of the Geological Society, London* **144**, 299–307.

Mecklenburgh, J. (2000). Deformation of partially molten synthetic granite. Ph.D. thesis, University of Manchester, 135 pp.

Milord, I., Sawyer, E. W. & Brown, M. (2001). Formation of diatexite migmatites and granite magma during anatexis of metasedimentary rocks: an example from St. Malo, France. *Journal of Petrology* **42**, 487–505.

Mo, X., Carmichael, I. S. E., Rivers, M. & Stebbins, J. (1982). The partial molar volume of Fe_2O_3 in multicomponent silicate liquids and the pressure dependence of oxygen fugacity in magmas. *Mineralogical Magazine* **45**, 237–245.

Munro, M. (1970). A reassessment of the 'younger' basic rocks between Huntly and Portsoy based on new borehole evidence. *Scottish Journal of Geology* **6**, 41–52.

Munro, M. (1984). Cumulate relations in the 'Younger Basic' masses of the Huntly–Portsoy area, Grampian Region. *Scottish Journal of Geology* **20**, 343–359.

Nichols, G. T., Berry, R. F. & Green, D. H. (1992). Internally consistent gahnitic spinel–cordierite–garnet equilibria in the FMASHZn system: geothermometry and applications. *Contributions to Mineralogy and Petrology* **111**, 362–377.

Nyman, M. W., Pattison, D. R. M. & Ghent, E. D. (1995). Melt extraction during formation of K-feldspar + sillimanite migmatites, west of Revelstoke, British Columbia. *Journal of Petrology* **36**, 351–372.

Oliver, G. J. H., Chen, F., Buchwaldt, R. & Hegner, E. (2000). Fast tectonometamorphism and exhumation in the type area of the Barrovian and Buchan zones. *Geology* **28**, 459–462.

Olsen, S. N. (1982). Open- and closed-system migmatites in the Front Range, Colorado. *American Journal of Science* **282**, 1596–1622.

Olsen, S. N. (1983). A quantitative approach to mass balance in migmatites. In: Atherton, M. P. & Gribble, C. D. (eds) *Migmatites, Melting and Metamorphism*. Nantwich: Shiva, pp. 201–233.

Pankhurst, R. J. (1969). Strontium isotope studies applied to petrogenesis in the basic igneous province of north-east Scotland. *Journal of Petrology* **10**, 116–145.

Pankhurst, R. J. (1970). The geochronology of the basic igneous complexes. *Scottish Journal of Geology* **6**, 83–107.

Pankhurst, R. J. (1974). Rb–Sr whole-rock chronology of Caledonian events in northeast Scotland. *Geological Society of America Bulletin* **85**, 345–350.

Patiño Douce, A. E. (1993). Titanium substitution in biotite: an empirical model with applications to thermometry, O_2 and H_2O barometries, and consequences for biotite stability. *Chemical Geology* **108**, 133–162.

Patiño Douce, A. E. & Beard, J. S. (1996). Effects of P, $f(O_2)$ and Mg/Fe ratio on dehydration melting of model metagraywackes. *Journal of Petrology* **37**, 999–1024.

Patiño Douce, A. E. & Johnston, A. D. (1991). Phase equilibria and melt productivity in the pelitic system: implications for the origins of peraluminous granitoids and aluminous granulites. *Contributions to Mineralogy and Petrology* **107**, 202–218.

Pattison, D. R. M. & Harte, B. (1988). Evolution of structurally contrasting anatectic migmatites in the 3 kbar Ballachulish aureole, Scotland. *Journal of Metamorphic Geology* **6**, 475–494.

Pattison, D. R. M. & Tracy, R. J. (1991). Phase equilibria and thermobarometry of metapelites. In: Kerrick, D. M. (ed.) *Contact Metamorphism. Mineralogical Society of America, Reviews in Mineralogy* **26**, 105–206.

Petford, N. J., Kerr, R. C. & Lister, J. R. (1993). Dyke transport of granitoid magmas. *Geology* **21**, 845–848.

Petford, N. J., Lister, J. R. & Kerr, R. C. (1994). The ascent of felsic magma in dykes. *Lithos* **32**, 161–168.

Pickering, J. M. & Johnston, A. D. (1998). Fluid-absent melting behavior of a two-mica metapelite. *Journal of Petrology* **39**, 1787–1804.

Pidgeon, R. T. & Aftalion, M. (1978). Cogenetic and inherited zircon U–Pb systems in granites: Palaeozoic granites of Scotland and England. In: Bowes, D. R. & Leake, B. E. (eds) *Crustal Evolution in Northwest Britain and Adjacent Regions. Geological Journal Special Issue* **10**, 183–220.

Powell, R. & Downes, J. (1990). Garnet porphyroblast-bearing leucosomes in metapelites: mechanisms, phase diagrams, and an example from Broken Hill, Australia. In: Ashworth, J. R. & Brown, M. (eds) *High-Temperature Metamorphism and Crustal Anatexis*. London: Unwin Hyman, pp. 105–123.

Powell, R. & Holland, T. J. B. (1988). An internally consistent thermodynamic dataset with uncertainties and correlations: 3. Application methods, worked examples and a computer program. *Journal of Metamorphic Geology* **6**, 173–204.

Powers, R. E. & Bohlen, S. R. (1985). The role of synmetamorphic igneous rocks in the metamorphism and partial melting of metasediments, Northwest Adirondacks. *Contributions to Mineralogy and Petrology* **90**, 401–409.

Read, H. H. (1919). The two magmas of Strathbogie and lower Banffshire. *Geological Magazine* **56**, 364–371.

Read, H. H. (1923*a*). *The Geology of the Country around Banff, Turriff and Huntly. Geological Survey of Scotland Memoir*. Edinburgh: British Geological Survey, HMSO, 240 pp.

Read, H. H. (1923*b*). The petrology of the Arnage district in Aberdeenshire: a study of assimilation. *Quarterly Journal of the Geological Society of London* **79**, 446–484.

Read, H. H. (1935). The gabbros and associated xenolithic complexes of the Haddo House district, Aberdeenshire. *Quarterly Journal of the Geological Society of London* **91**, 591–635.

Read, H. H. (1952). Metamorphism and migmatization in the Ythan valley, Aberdeenshire. *Transactions of the Edinburgh Geological Society* **15**, 265–279.

Read, H. H. (1961). Aspects of Caledonian magmatism in Britain. *Liverpool and Manchester Geological Journal* **2**, 653–683.

Rogers, G., Paterson, B. A., Dempster, T. J. & Redwood, S. D. (1994). U–Pb geochronology of the Newer Gabbros, NE Grampians (unpublished conference abstract). *Caledonian Terrane Relationships in Britain*. Keyworth: British Geological Survey.

Rudnick, R. (1990). Continental crust—growing from below. *Nature* **347**, 711–712.

Rutter, E. H. (1997). The influence of deformation on the extraction of crustal melts: a consideration of the role of melt-assisted granular flow. In: Holness, M. B. (ed.) *Deformation-enhanced Fluid Transport in the Earth's Crust and Mantle*. London: Chapman and Hall, pp. 82–110.

Rutter, E. H. & Neumann, D. H. K. (1995). Experimental deformation of partially molten Westerly granite under fluid-absent conditions, with implications for the extraction of granitoid magmas. *Journal of Geophysical Research* **100**, 15697–15715.

Sawyer, E. W. (1994). Melt segregation in the continental crust. *Geology* **22**, 1019–1022.

Sawyer, E. W. (2001). Melt segregation in the continental crust: distribution and movement of melt in anatectic rocks. *Journal of Metamorphic Geology* **19**, 291–310.

Scaillet, B., Holtz, F. & Pichavant, M. (1998). Phase equilibrium constraints on the viscosity of silicic magmas: 1. Volcanic–plutonic association. *Journal of Geophysical Research* **B103**, 27257–27266.

Schnetger, B. (1994). Partial melting during the evolution of the amphibolite- to granulite-facies gneisses of the Ivrea Zone, northern Italy. *Chemical Geology* **113**, 71–101.

Schreyer, W. & Yoder, H. S. (1964). The system Mg-cordierite–H_2O and related rocks. *Neues Jahrbuch für Mineralogie, Abhandlungen* **101**, 271–342.

Shackleton, R. M. (1948). Overturned rhythmic banding in the Huntly gabbro of Aberdeenshire. *Geological Magazine* **85**, 358–360.

Shaw, H. R. (1965). Comments on viscosity, crystal settling, and convection in granitic magmas. *American Journal of Science* **263**, 120–152.

Simakin, A. & Talbot, C. (2001). Tectonic pumping of pervasive granitic melts. *Tectonophysics* **332**, 387–402.

Sleep, N. H. (1988). Tapping of melt by veins and dykes. *Journal of Geophysical Research* **B93**, 10255–10272.

Solar, G. & Brown, M. (2001). Petrogenesis of migmatites in Maine, USA: possible sources of peraluminous leucogranite in plutons? *Journal of Petrology* **42**, 789–823.

Srogi, L., Wagner, M. E. & Lutz, T. M. (1993). Dehydration partial melting and disequilibrium in the granulite-facies Wilmington Complex, Pennsylvania–Delaware piedmont. *American Journal of Science* **293**, 405–462.

Stevens, G. (1995). Compositional controls on partial melting in high-grade metapelites: a petrological and experimental study. Ph.D. thesis, University of Manchester.

Stevens, G. & Clemens, J. D. (1993). Fluid-absent melting and the role of fluids in the lithosphere: a slanted summary? *Chemical Geology* **108**, 1–17.

Stevens, G., Clemens, J. D. & Droop, G. T. R. (1997). Melt production during granulite-facies anatexis: experimental data from 'primitive' metasedimentary protoliths. *Contributions to Mineralogy and Petrology* **128**, 352–370.

Stewart, F. H. (1946). The gabbroic complex of Belhelvie in Aberdeenshire. *Quarterly Journal of the Geological Society of London* **102**, 465–498.

Stewart, F. H. & Johnson, M. R. W. (1960). The structural problem of the younger gabbros of north-east Scotland. *Transactions of the Royal Society of Edinburgh* **18**, 104–112.

Thompson, A. B. (1982). Dehydration melting of pelitic rocks and the generation of H_2O-undersaturated granitic liquids. *American Journal of Science* **282**, 1567–1595.

Thompson, A. B. (1990). Heat, fluids and melting in the granulite facies. In: Vielzeuf, D. & Vidal, P. (eds) *Granulites and Crustal Differentiation. NATO ASI Series*. Dordrecht: Kluwer Academic, pp. 37–58.

Treagus, J. E. & Roberts, J. L. (1981). The Boyndie Syncline, a D1 structure in the Dalradian of Scotland. *Geological Journal* **16**, 125–135.

Ulmer, G. C. (ed.) (1971). *Research Techniques for High Pressure and High Temperature*. New York: Springer.

van der Molen, I. & Paterson, M. S. (1979). Experimental deformation of partially-melted granite. *Contributions to Mineralogy and Petrology* **70**, 299–318.

Vernon, R. H. (1987). Oriented growth of sillimanite in andalusite, Placitos–Juan Tabo area, New Mexico, USA. *Canadian Journal of Earth Sciences* **24**, 580–590.

Vernon, R. H. & Collins, W. J. (1988). Igneous microstructures in migmatites. *Geology* **16**, 1126–1129.

Vielzeuf, D. & Holloway, J. R. (1988). Experimental determination of the fluid-absent melting reactions in the pelitic system. Consequences for crustal differentiation. *Contributions to Mineralogy and Petrology* **98**, 257–276.

Vielzeuf, D. & Montel, J.-M. (1994). Partial melting of metagreywackes. 1. Fluid-absent experiments and phase relationships. *Contributions to Mineralogy and Petrology* **117**, 375–393.

Vielzeuf, D., Clemens, J. D., Pin, C. & Moinet, E. (1990). Granites, granulites and crustal differentiation. In: Vielzeuf, D. & Vidal, P. (eds) *Granulites and Crustal Differentiation. NATO ASI Series*. Dordrecht: Kluwer Academic, pp. 59–86.

Vigneresse, J. L., Barbey, P. & Cuney, M. (1996). Rheological transitions during partial melting and crystallization with application to felsic magma segregation and transfer. *Journal of Petrology* **37**, 1579–1600.

Vry, J. K., Brown, P. E. & Valley, J. W. (1990). Cordierite volatile contents and the role of CO_2 in high-grade metamorphism. *American Mineralogist* **75**, 71–88.

Wadsworth, W. J. (1982). The basic plutons. In: Sutherland, D. (ed.) *Igneous Rocks of the British Isles*. Chichester: John Wiley, pp. 135–148.

Wadsworth, W. J. (1986). Silicate mineralogy in the later fractionation stages of the Insch intrusion, N. E. Scotland. *Mineralogical Magazine* **50**, 583–595.

Wadsworth, W. J. (1988). Silicate mineralogy of the Middle Zone cumulates and associated gabbroic rocks from the Insch intrusion, N. E. Scotland. *Mineralogical Magazine* **52**, 309–322.

Wadsworth, W. J., Stewart, F. H. & Rothstein, A. T. V. (1966). Cryptic layering in the Belhelvie intrusion, Aberdeenshire. *Scottish Journal of Geology* **2**, 54–66.

Waters, D. J. (1988). Partial melting and the formation of granulite-facies assemblages in Namaqualand, South Africa. *Journal of Metamorphic Geology* **6**, 387–404.

Waters, D. J. & Whales, C. J. (1984). Dehydration melting and the granulite transition in metapelites from southern Namaqualand, S. Africa. *Contributions to Mineralogy and Petrology* **88**, 269–275.

Watson, E. B. (1982). Basalt contamination by continental crust: some experiments and models. *Contributions to Mineralogy and Petrology* **80**, 73–87.

Watt, W. R. (1914). The geology of the country around Huntly, Aberdeenshire. *Quarterly Journal of the Geological Society of London* **70**, 266–293.

Weber, C., Barbey, P., Cuney, M. & Martin, H. (1985). Trace element behaviour during migmatisation: evidence for a complex melt–residuum–fluid interaction in the St. Malo migmatitic dome (France). *Contributions to Mineralogy and Petrology* **90**, 52–62.

Weedon, D. S. (1970). The ultrabasic/basic rocks of the Huntly region. *Scottish Journal of Geology* **6**, 26–40.

White, R. W., Powell, R. & Holland, T. J. B. (2001). Calculation of partial melting equilibria in the system Na_2O–CaO–K_2O–FeO–MgO–Al_2O_3–SiO_2–H_2O (NCKFMASH). *Journal of Metamorphic Geology* **19**, 139–153.

Wickham, S. M. (1987). The segregation and emplacement of granitic magmas. *Journal of the Geological Society, London* **144**, 281–297.

Wood, B. J. & Banno, S. (1972). Garnet–orthopyroxene and orthopyroxene–clinopyroxene equilibria in the system CaO–MgO–Al_2O_3–SiO_2. *Geochimica et Cosmochimica Acta* **48**, 299–311.